About the unfolding of a Hopf-zero singularity

Freddy Dumortier
Universiteit Hasselt
Campus Diepenbeek
Agoralaan-Gebouw D, B-3590, Diepenbeek, Belgium
E-mail: freddy.dumortier@uhasselt.be

Santiago Ibáñez
Departamento de Matemáticas
Universidad de Oviedo
Avda. Calvo Sotelo s/n, 33007 Oviedo, Spain
E-mail: mesa@uniovi.es

Hiroshi Kokubu
Department of Mathematics/JST-CREST
Kyoto University
Kyoto 606-8502, Japan
E-mail: kokubu@math.kyoto-u.ac.jp

Carles Simó
Departament de Matemàtica Aplicada i Anàlisi
Universitat de Barcelona
Gran Via, 585, 08071 Barcelona, Spain
E-mail: carles@maia.ub.es

September 18, 2012

Abstract

We study arbitrary generic unfoldings of a Hopf-zero singularity of codimension two. They can be written in the following normal form:

$$\begin{cases} x' = -y + \mu x - axz + A(x, y, z, \lambda, \mu) \\ y' = x + \mu y - ayz + B(x, y, z, \lambda, \mu) \\ z' = z^2 + \lambda + b(x^2 + y^2) + C(x, y, z, \lambda, \mu), \end{cases}$$

where A, B, C are C^∞ or C^ω and of order $O(\|(x, y, z, \lambda, \mu)\|^3)$. Moreover we focus on the most interesting case, namely, the topological type of codimension two characterized by the open conditions $a > 0$ and $b > 0$.

At second order the above family is integrable for $\mu = 0$ and, when $\lambda < 0$, there exist on the vertical axis two saddle-focus equilibrium points with different stability indices. Their respective two-dimensional invariant manifolds coincide and form an ellipsoid. Inside, the equilibrium points are connected by a heteroclinic orbit along the vertical axis. Such configuration can be destroyed by higher order terms and therefore homoclinic and heteroclinic orbits can appear. The saddle-focus homoclinic orbits will satisfy the Shilnikov conditions for $0 < a < 2$ and, in such a case, chaotic dynamics should be present in the system for some parameter values.

The determinacy of the splitting function is a very involved problem which has been tackled by several authors. The difficulty lies in the fact that some higher order terms have an exponentially small effect in the splitting. Moreover no formula, valid for any generic unfolding, for the coefficients in the leading terms of the splitting function is available. In fact, unless we use the exact form of the vector fields we cannot expect to get such a formula. No truncation can provide information about exponentially small phenomena. A different question is to know what happens in general, that is, the behaviour out of a set of families of large codimension.

In this paper we work with meaningful expressions for the splitting functions. They are supported by partial theoretical results present in the literature and also by numerical results. We generically assume that the leading coefficients do not vanish and explore the dynamical consequences of certain additional mild conditions. We will also pay attention to the so-called Michelson system, a specific unfolding of the Hopf-zero singularity consisting of volume preserving vector fields, and hence leading to measure preserving families of diffeomorphisms for suitable Poincaré maps. Michelson system is related to the study of the unfolding of the three-dimensional nilpotent singularity of codimension three and as well as to the Kuramoto-Shivashinsky equation. Numerical results supporting the validity of the splitting assumptions and showing several aspects of the dynamics are also presented.

Contents

1 Introduction

This paper deals with C^∞ and C^ω unfoldings of singularities on $\mathbb{R}^3$ whose linear part is conjugated to

$$x' = -\omega y, \quad y' = \omega x, \quad z' = 0, \tag{1.1}$$

with $\omega > 0$. We refer to them as *Hopf-zero singularities*, *HZ* singularities in the sequel. Although they have been widely studied, some problems related with their unfoldings still remain unsolved.

1.1 Hopf-zero singularities of codimension two

Classification of *HZ* singularities was first done in [46]. Up to C^∞-equivalence the 2-jet of any singularity with linear part (1.1) can be written in the following normal form:

$$\begin{cases} x' = -y - axz \\ y' = x - ayz \\ z' = cz^2 + b(x^2 + y^2). \end{cases}$$

The degeneracy conditions imposed on the linear part and the open conditions $a \neq 0$, $b \neq 0$ and $c \neq 0$ characterize a stratum of codimension two in the space of germs of singularities of vector fields on $\mathbb{R}^3$. Moreover coefficient c can be normalized by a scaling of coordinates and we can write the above system as:

$$\begin{cases} x' = -y - axz \\ y' = x - ayz \\ z' = z^2 + b(x^2 + y^2). \end{cases} \tag{1.2}$$

F. Takens proved in [46] that *HZ* singularities of codimension two are 2-jet determined. He used the notion of *weak* C^0-equivalence but in fact one can show that they are 2-jet determined with respect to the C^0 equivalence (see [14]). There are six topological types of *HZ* singularities of codimension two. However we are only interested in the topological type characterized by the conditions $a > 0$ and $b > 0$. We will refer to it as *HZ** singularity.

1.2 Unfoldings

Generic unfoldings of *HZ* singularities of codimension two were first studied by Guckenheimer [22] and Gavrilov [20]. Any of such unfoldings can be written, at the 2-jet level, in the following normal form:

$$\begin{cases} x' = -y + \mu x - axz \\ y' = x + \mu y - ayz \\ z' = \lambda + z^2 + b(x^2 + y^2) \end{cases} \tag{1.3}$$

and taking the cylindrical coordinates we obtain:

$$\begin{cases} r' = \mu r - arz \\ z' = \lambda + z^2 + br^2. \end{cases} \tag{1.4}$$

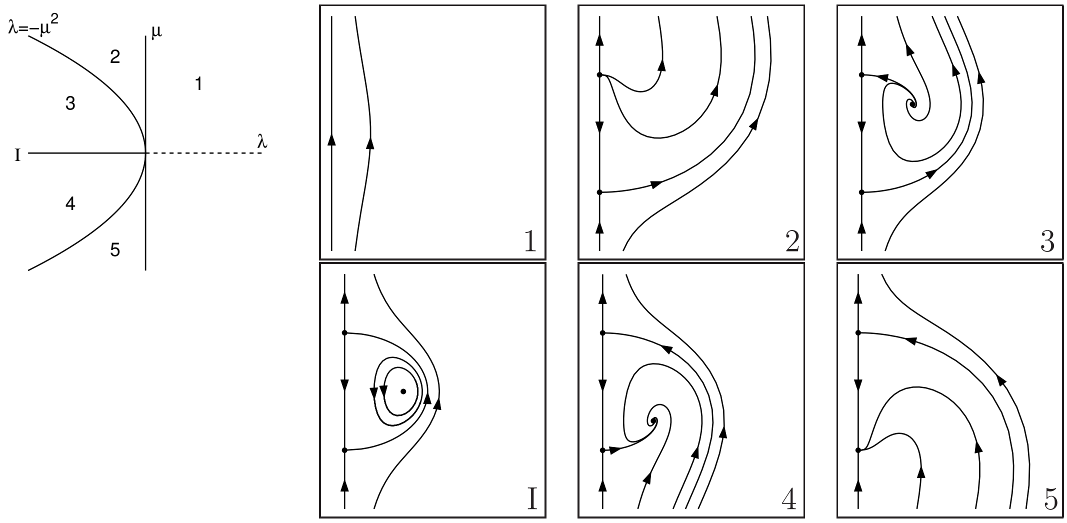

Figure 1: Bifurcation diagram for family (1.4) for $a > 0$ and $b > 0$.

The bifurcation diagram of family (1.4) for $a > 0$ and $b > 0$ is shown in Figure 1. The most remarkable feature is that, when $\mu = 0$, the function

$$H(r, z) = r^{\frac{2}{a}} \left(\lambda + z^2 + \frac{b}{1+a} r^2 \right)$$

becomes a first integral of the family (1.4). The phase portrait when $\lambda < 0$ is depicted in Figure 1 (see case I). The invariant manifolds at the equilibrium points on the vertical axis form a heteroclinic cycle whose interior is covered by a continuum of periodic orbits. Consequently, for the three-dimensional vector field, the two-dimensional invariant manifolds of the equilibrium points form an ellipsoid. Inside, two branches of the one-dimensional invariant manifolds are coincident along the vertical axis.

The integrable structure can be destroyed under the effect of higher order terms, even if the rotational symmetry is still preserved. Nevertheless, in that case, under generic conditions (see [23, 32]), one can prove that there exists a bifurcation curve where system shows again an invariant ellipsoid formed by the two-dimensional invariant manifolds of the equilibrium points at the vertical axis.

For non-rotationally symmetric unfoldings of the HZ^* singularity the situation is completely different. The configuration consisting of an invariant ellipsoid of orbits connecting two equilibrium points and the additional inner heteroclinic connection (see Figure 1, Case I) is highly degenerate. Generically, the two-dimensional invariant manifolds will intersect transversally and the codimension two connection between the one-dimensional invariant manifolds will break. The splitting of the invariant manifolds makes homoclinic orbits possible. Nevertheless the study of the splitting turns out to be a very involved matter.

As we will see in Section 2, any generic unfolding of the HZ^* singularity can be written, for $\lambda < 0$, as

$$\left\{ \begin{array}{l} \bar{x}' = -\frac{1}{\varepsilon}\bar{y} + \bar{\mu}\bar{x} - a\bar{x}\bar{z} + O(\varepsilon) \\ \bar{y}' = \frac{1}{\varepsilon}\bar{x} + \bar{\mu}\bar{y} - a\bar{y}\bar{z} + O(\varepsilon) \\ \bar{z}' = \bar{z}^2 - 1 + b(\bar{x}^2 + \bar{y}^2) + O(\varepsilon), \end{array} \right.$$

for certain specific functions $O(\varepsilon)$ to be made precise in Section 2.

1.3 Purpose of the paper

Goal of the paper is to present new techniques to study global bifurcations from *HZ* singularities, as well as their important dynamical consequences in general unfoldings of the HZ^* singularity. The methods we present here are (A) *the blow-up method and a related invariant manifold theory*, and (B) the new approach to the *splitting functions* of the invariant manifolds, both in the context of unfoldings of the HZ^* singularity. The former one, (A), is used to provide with a general criterion (Theorem 3.3) for the existence of Shilnikov homoclinic orbits in an arbitrary unfolding of the HZ^* singularity, and the latter (B) is used to give a more detailed structure of the Shilnikov homoclinic bifurcation set in the unfoldings (Theorem 3.13).

Similar results about Bykov cycles (see Definition 3.6) hold for general reversible systems unfolding the HZ^* singularity (see Theorem 3.7 and Remark 3.20). Let us for the rest of this section concentrate on the Shilnikov phenomena.

The motivation of this study comes from the fact that there is no general criterion known, before this paper, for the existence of the Shilnikov homoclinic bifurcation in an *arbitrary* unfolding from the HZ^* singularity. To make it clear we need to comment several contributions already available in the literature. Indeed, geometrical arguments were provided in [23] to support the possibility of existence. In [19] the author considers a class of unfoldings of the form $X_2 + \varepsilon Y$ where $X_2 = X_2(x, y, z, \lambda, \mu)$ is the family of vector fields given by the equations (1.3), ε is a small parameter and $Y = Y(x, y, z)$ is independent of parameters and only contains third order terms. Under these conditions it is possible to conclude the existence of exponentially small splitting functions and show the existence of Shilnikov homoclinic orbits. In [12] the authors show that the same analysis can be extended to the case of Y analytic. Nevertheless, as we will see in this paper, unfoldings in general cannot be written in that way.

In contrast, in [5], the authors prove that for every generic unfolding of a HZ^* singularity there exists a flat perturbation leading to a family exhibiting the Shilnikov phenomenon. They also prove that the phenomenon is persistent in the strong C^1-Whitney topology and dense in the C^∞-topology. All these results have been extended to time reversible unfoldings in [33], where it is proved that the phenomenon is generic in the C^∞ topology. As such there seems to be plenty of unfoldings exhibiting the Shilnikov phenomenon. Nevertheless their results do not provide any criterion for the existence of Shilnikov homoclinic orbits because their arguments are related to flat perturbations.

In this paper, we would like to propose a general criterion for the existence of Shilnikov homoclinic orbits, as well as a more precise description of the Shilnikov bifurcation set. We shall give in the following a more precise overview of the methods and the results given in the paper, together with some related known results in the literature.

(A) *Blow-up and invariant manifold for existence criterion for the Shilnikov homoclinic orbits in an unfolding of HZ^* singularity*

Usual blow-up techniques can be applied to study any general unfolding of the HZ^* singularity. Nevertheless we will see that introducing a scaling parameter ε we obtain either a singular perturbation problem with a pure rotation for $\varepsilon = 0$ or a family with rotation speed tending to ∞ as $\varepsilon \to 0$. Using one or the other approach, there is no clear limit for the invariant manifolds of the equilibrium points as $\varepsilon \to 0$. In fact it is not clear whether the notion of splitting distance is meaningful in the context of this kind of unfoldings. However we can apply the results in [3, 4] to prove that such invariant manifolds have a limit position, given by the corresponding invariant manifolds of the equilibrium points at the 2-jet level, as the scaling parameter tends to 0, whenever we consider restrictions to $\{\bar{z} \geq 0\}$ or $\{\bar{z} \leq 0\}$. As a consequence splitting functions are well defined for any generic unfolding of a HZ^* singularity. We believe this is a new result.

Before entering discussions about splitting functions we will introduce the notion of forward and backward trapping which plays a central role to give an existence criterion for the Shilnikov homoclinic orbits in an unfolding of HZ^* singularity. More precisely, under suitable assumptions, if one has a continuous path in the parameter space of a general unfolding joining parameter points in forward and backward trapping, one must have a parameter value in the path that corresponds to the existence of Shilnikov homoclinic orbit. See Theorem 3.3 for a more detailed statement. Notice that results in [3, 4] are essential for the notion of trapping.

(B) *Splitting function and bifurcation set for the Shilnikov homoclinic orbits in an unfolding of HZ^* singularity*

Knowing that splitting functions are well defined for any general unfolding we give formulas for the splitting functions. In fact, the splitting function for the one-dimensional invariant manifolds is given in [2] and we shall make use of it. We also give a formula for the splitting of the two-dimensional invariant manifolds. In such formulas we assume that the contribution of the terms which do not preserve the rotationally symmetry is not only beyond all orders but are indeed exponentially small in the scaling parameter. Results in [2] show that the splitting function of the one-dimensional invariant manifolds is also exponentially small. All our assumptions will be supported by a theoretical discussion and also by thorough numerical experiments. Under mild conditions on the splitting functions we are able to provide a deeper understanding of the bifurcation set for the Shilnikov homoclinic orbits in an unfolding of HZ^* singularity. See Theorem 3.13. The result can be applied to general one-parameter unfoldings and shows, under suitable hypotheses, the existence of a sequence of Shilnikov homoclinic bifurcation points accumulating to 0.

1.4 The nilpotent singularity of codimension three and the Michelson system

In this paper we will also pay attention to a specific quadratic family of three-dimensional vector fields, which contains a HZ^* singularity, and which plays an essential role in the study of generic unfoldings of the three-dimensional nilpotent singularity of codimension three. In the study of such unfolding (see details in [13], [15] and [16]) we find the following limit family after an appropriate rescaling:

$$\begin{aligned} x' &= y \\ y' &= z \\ z' &= \bar{\lambda} + \bar{\mu} y + \bar{\nu} z + x^2, \end{aligned} \tag{1.5}$$

with $\bar{\lambda}^2 + \bar{\mu}^2 + \bar{\nu}^2 = 1$ and (x, y, z) in an arbitrarily large compact domain $K \subset \mathbb{R}^3$. When $(\bar{\lambda}, \bar{\mu}, \bar{\nu}) = (0, -1, 0)$ the above system has a HZ^* singularity at the origin. The bifurcation diagram of the family (1.5) around this point is a crucial ingredient for understanding the unfolding of the nilpotent singularity. It easily follows that the family:

$$\begin{aligned} x' &= y \\ y' &= z \\ z' &= \lambda - y + \nu z + x^2, \end{aligned} \tag{1.6}$$

with $\lambda \in \mathbb{R}$ and $\nu \in \mathbb{R}$ is equivalent, after an appropriate rescaling, to (1.5) with $\bar{\mu} < 0$.

Important to notice is that the subfamily obtained from (1.6) by taking $\nu = 0$ and $\lambda \leq 0$ has its own relevance. Rescaling by $x = -\bar{x}/2$, $y = -\bar{y}/2$ and $z = -\bar{z}/2$ we obtain, preserving the notation for variables,

$$\begin{aligned} x' &= y \\ y' &= z \\ z' &= c^2 - \tfrac{x^2}{2} - y, \end{aligned} \tag{1.7}$$

where $c^2 = -2\lambda$. The above family is known in the literature as the *Michelson system* and it appears as the equation for travelling wave solutions of a non-linear PDE called the Kuramoto-Sivashinsky equation:

$$u_t + u_{xxxx} + u_{xx} + \frac{1}{2}u_x^2 = 0, \quad (t \geq 0, x \in \mathbb{R}). \tag{1.8}$$

See [30] or [37] for precise derivation of (1.7) from the PDE. There is a huge number of papers devoted to the dynamics and bifurcations of the Michelson system (e.g. [1, 15, 16, 25, 26, 27, 28, 29, 30, 31, 33, 34, 36, 37, 39, 47, 49, 50]).

Remark 1.1 Let us point out, for future reference, some basic properties of (1.7):

- Since the divergence is identically zero, the family is volume-preserving.
- The family is reversible, namely, it is invariant under the involution $R : (x, y, z) \mapsto (-x, y, -z)$ and the time reverse $t \mapsto -t$.
- For $c > 0$ there are only two equilibrium points at

  $$P_{\pm} = (\pm\sqrt{2}c, 0, 0),$$

  both are of saddle-focus type with $\dim W^u(P_+) = \dim W^s(P_-) = 2$.

As already mentioned the system (1.6) with $\nu = 0$ and $\lambda \leq 0$ corresponds to the Michelson system (1.7) with $c^2 = -2\lambda$. In that sense the system (1.6) is the result of adding some constant divergence to the Michelson system. Due to that reason, in this paper we will refer to the system (1.6) as the *extended Michelson system*.

1.5 Plan of the paper

In Section 2 we will provide the reduction to normal form of unfoldings of Hopf-zero singularities and explain how far the blow-up techniques can be used. At the end of Section 2 we will show that family (1.6), and therefore Michelson system too, is indeed an unfolding of a HZ^* singularity.

In Section 3 we will see that results in [3, 4] show that, after scaling, the limit position of the invariant manifolds is indeed determined by the integrable family (1.4) and we provide sufficient conditions for the existence of Shilnikov homoclinic orbits and also the accumulation of a certain type of heteroclinic cycles in an unfolding of the singularity. We will provide formulas, supported by theoretical arguments and numerical experiments, for the splitting functions of the two-dimensional invariant manifolds. Moreover we will refer to [2] with regards to the splitting of the one-dimensional invariant manifolds. Let us mention that [45] contains an argument showing that upper bounds for the splitting are close to the right value in certain families of area preserving maps. The Michelson system will be treated specifically since more precise results for the splittings are already present in the literature (see [39, 1, 49]). With these formulas we will provide results explaining, under mild assumptions, the structure of the bifurcation set of Shilnikov homoclinic orbits.

Section 4 deals entirely with the Michelson system and extended Michelson system. First we briefly summarize the most relevant known results. Application of the theoretical results presented in Section 3 is discussed and a thorough numerical exploration of dynamics is also provided.

Section 5 contains a final discussion about the state of the problem and the lines for future research.

Remark 1.2 Bifurcations of *Hopf-saddle-node* fixed points for three-dimensional diffeomorphisms, that is, with spectrum $\{e^{\mathrm{i}\omega}, e^{-\mathrm{i}\omega}, 1\}$, have been studied in [7, 8, 9, 10, 11, 48] with the motivation of their occurrence in climatological models with seasonal forcing (see [6]). Such models lead to three-dimensional vector fields with periodic forcing terms and diffeomorphisms are given by Poincaré maps. The unfolding exhibits a very rich dynamics. Particularly, one finds Ruelle-Takens routes to turbulence. For vector fields it means that in a suitable open set of parameters there exist strange attractors arising after a third Hopf bifurcation, that is, a periodic orbit emerges in a Hopf bifurcation and later a sequence of two Neimark-Sacker bifurcations leads to a three-dimensional torus.

2 Normal forms and blow-ups

2.1 Normal forms

Take an arbitrary two-parameter unfolding of a HZ^* singularity having a 2-jet which is generic with respect to parameters and variables; it can be either C^∞ or C^ω. After a C^∞ (resp. C^ω) diffeomorphic change in the parameter plane, the choice of appropriate C^∞ (resp. C^ω) coordinates and a time rescaling one can suppose that the two-parameter family looks like:

$$\begin{cases} x' = -y + \mu x - axz + A(x, y, z, \lambda, \mu) \\ y' = x + \mu y - ayz + B(x, y, z, \lambda, \mu) \\ z' = z^2 + \lambda + b(x^2 + y^2) + C(x, y, z, \lambda, \mu) \end{cases} \tag{2.1}$$

where A, B, C are C^∞ or C^ω depending on the regularity of the original family and A, B, and C are $O(\|(x, y, z, \lambda, \mu)\|^3)$. The conditions given for A, B and C are maybe not the best that one can obtain but sufficient for our purpose.

If necessary we can refine this normal form (in a C^∞ or a C^ω way) to:

$$\begin{cases} x' = -y + \mu x - a(\lambda, \mu)xz + f_1(x^2 + y^2, z, \lambda, \mu)x + g_1(x, y, z, \lambda, \mu) \\ y' = x + \mu y - a(\lambda, \mu)yz + f_1(x^2 + y^2, z, \lambda, \mu)y + g_2(x, y, z, \lambda, \mu) \\ z' = z^2 + \lambda + b(\lambda, \mu)(x^2 + y^2) + f_3(x^2 + y^2, z, \lambda, \mu) + g_3(x, y, z, \lambda, \mu) \end{cases} \tag{2.2}$$

with $g_i = O(\|(x, y, z, \lambda, \mu)\|^N)$, for any a priori chosen N, $i = 1, 2, 3$, and $f_1(0, 0, \lambda, \mu) = \frac{\partial f_1}{\partial z}(0, 0, \lambda, \mu) = 0$; $a(0, 0) = a$ and $b(0, 0) = b$. We could even take $N = +\infty$, but then the normal form will in any case only be C^∞, even if we start with a C^ω unfolding.

2.2 Blow-up

We intend to study such a family (2.1) for parameters

$$(\lambda, \mu) \quad = \quad (-\varepsilon^2, \varepsilon\bar{\mu}). \tag{2.3}$$

with $\bar{\mu} \in [-\bar{\mu}_0, \bar{\mu}_0]$ for some $0 < \bar{\mu}_0 < a$, where $\bar{\mu}_0$ might be submitted to some extra restrictions to be made precise later on.

Let us for the moment continue with the expression (2.1) and only use (2.2) where necessary. Applying (2.3) to (2.1) gives:

$$\begin{cases} x' = -y + \varepsilon\bar{\mu}x - axz + A(x, y, z, \varepsilon^2, \varepsilon\bar{\mu}) \\ y' = x + \varepsilon\bar{\mu}y - ayz + B(x, y, z, \varepsilon^2, \varepsilon\bar{\mu}) \\ z' = z^2 - \varepsilon^2 + b(x^2 + y^2) + C(x, y, z, \varepsilon^2, \varepsilon\bar{\mu}). \end{cases} \tag{2.4}$$

For $\varepsilon > 0$ we now rescale (2.4) by means of

$$x = \varepsilon\bar{x}, \quad y = \varepsilon\bar{y}, z = \varepsilon\bar{z} \tag{2.5}$$

and get

$$\begin{cases} \bar{x}' = -\bar{y} + \varepsilon\bar{\mu}\bar{x} - \varepsilon a\bar{x}\bar{z} + O(\varepsilon^2) \\ \bar{y}' = \bar{x} + \varepsilon\bar{\mu}\bar{y} - \varepsilon a\bar{y}\bar{z} + O(\varepsilon^2) \\ \bar{z}' = \varepsilon\bar{z}^2 - \varepsilon + \varepsilon b(\bar{x}^2 + \bar{y}^2) + O(\varepsilon^2). \end{cases} \tag{2.6}$$

We could divide by ε, for $\varepsilon > 0$, and equally study

$$\widetilde{X}_{\varepsilon,\bar{\mu}} \begin{cases} \bar{x}' = -\frac{1}{\varepsilon}\bar{y} + \bar{\mu}\bar{x} - a\bar{x}\bar{z} + O(\varepsilon) \\ \bar{y}' = \frac{1}{\varepsilon}\bar{x} + \bar{\mu}\bar{y} - a\bar{y}\bar{z} + O(\varepsilon) \\ \bar{z}' = \bar{z}^2 - 1 + b(\bar{x}^2 + \bar{y}^2) + O(\varepsilon). \end{cases} \tag{2.7}$$

At the 2-jet level we can consider the two-dimensional limiting "reduced system" $Z_{\bar{\mu}}$, as introduced by Takens in [46], that we obtain by forgetting the rotational term and the $O(\varepsilon)$-terms.

$$Z_{\bar{\mu}} \begin{cases} \bar{r}' = \bar{\mu}\bar{r} - a\bar{r}\bar{z} \\ \bar{z}' = \bar{z}^2 - 1 + b\bar{r}^2, \end{cases} \tag{2.8}$$

with $\bar{r}^2 = \bar{x}^2 + \bar{y}^2$. The phase portraits are presented in Figure 2, depending on the value of $\bar{\mu}$. We are especially interested in the dynamics that $\widetilde{X}_{\varepsilon,\bar{\mu}}$ and equivalently $\varepsilon\widetilde{X}_{\varepsilon,\bar{\mu}}$ can have for $\bar{\mu} \sim 0$, hence for systems whose limiting system is the one represented in Figure 2 by $\bar{\mu} = 0$.

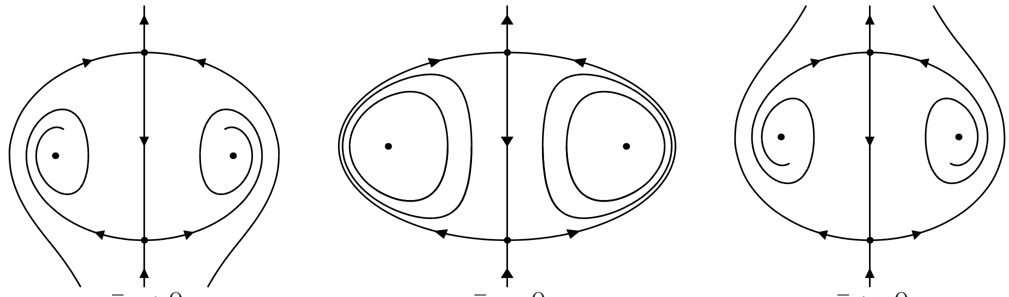

Figure 2: Phase portraits of the reduced vector field.

2.3 Analytic one-parameter unfoldings

As announced in the introduction we will also pay great attention to analytic one-parameter families unfolding the HZ^* singularity, presenting a very small friction. In terms of an analytic expression as in (2.1) we consider one-parameter subfamilies of (2.1) given by some analytic function

$$\mu = \mu(\lambda)$$

with $\mu(0) = 0$. Expression (2.1) changes into:

$$\begin{cases} x' = -y + \mu(\lambda)x - axz + A_1(x, y, z, \lambda) \\ y' = x + \mu(\lambda)y - ayz + B_1(x, y, z, \lambda) \\ z' = z^2 + \lambda + b(x^2 + y^2) + C_1(x, y, z, \lambda). \end{cases} \tag{2.9}$$

Since μ is no longer an independent parameter, it makes no longer sense to apply (2.3). In combination with (2.5) we make the following rescaling of the one-parameter family

$$(x, y, z, \lambda) = (\varepsilon\bar{x}, \varepsilon\bar{y}, \varepsilon\bar{z}, -\varepsilon^2)$$

leading to

$$\begin{cases} \bar{x}' = -\bar{y} - \varepsilon a\bar{x}\bar{z} + O(\varepsilon^2) \\ \bar{y}' = \bar{x} - \varepsilon a\bar{y}\bar{z} + O(\varepsilon^2) \\ \bar{z}' = \varepsilon\bar{z}^2 - \varepsilon + \varepsilon b(\bar{x}^2 + \bar{y}^2) + O(\varepsilon^2), \end{cases} \tag{2.10}$$

or equivalently

$$\widetilde{X}_\varepsilon \begin{cases} \bar{x}' = -\frac{1}{\varepsilon}\bar{y} - a\bar{x}\bar{z} + O(\varepsilon) \\ \bar{y}' = \frac{1}{\varepsilon}\bar{x} - a\bar{y}\bar{z} + O(\varepsilon) \\ \bar{z}' = \bar{z}^2 - 1 + b(\bar{x}^2 + \bar{y}^2) + O(\varepsilon). \end{cases} \tag{2.11}$$

There is now a unique limiting reduced system Z_0, as represented in the middle picture of Figure 2.

Remark 2.1 A natural question is the integrability of the normal form when higher order terms in the normal form are taken into account. It turns out that the resulting system is integrable if and only if the original vector field is volume preserving.

Remark 2.2 Note that all the normal forms obtained up to now are valid for any HZ singularity, not only for HZ^*.

2.4 Normal form for the extended Michelson system

To end this section let us show that the extended Michelson system (1.6) is indeed an unfolding of the HZ^* singularity.

Applying to (1.6) the linear change of coordinates $x = X + Z$, $y = Y + \lambda$, $z = -Z$, the following system is obtained:

$$\left\{\begin{array}{l} X' = \lambda - \nu Z + (X+Z)^2 \\ Y' = -Z \\ Z' = Y + \nu Z - (X+Z)^2. \end{array}\right.$$

Again we consider a linear change of coordinates $X = z$, $Y = x$, $Z = y$ leading to:

$$\left\{\begin{array}{l} x' = -y \\ y' = x + \nu y - (z+y)^2 \\ z' = \lambda - \nu y + (z+y)^2. \end{array}\right.$$

In order to reduce to a normal form, we introduce the complex coordinate $w = x + iy$. Then

$$\left\{\begin{array}{l} w' = iw + \frac{\nu}{2}(w-\bar{w}) - iz^2 - z(w-\bar{w}) + \frac{i}{4}(w-\bar{w})^2 \\ z' = \lambda + \frac{\nu}{2}i(w-\bar{w}) + z^2 - iz(w-\bar{w}) - \frac{1}{4}(w-\bar{w})^2. \end{array}\right.$$

Using such complex coordinate, the terms which satisfy the resonance conditions are $w^k\bar{w}^l z^m \frac{\partial}{\partial w}$ with $k - l + 1 = 0$ and $w^k\bar{w}^l z^m \frac{\partial}{\partial z}$ with $k - l = 0$. As a consequence, reducing the 2-jet to normal form we obtain:

$$\left\{\begin{array}{l} w' = iw + \frac{\nu}{2}w - zw + O(\|(w,\bar{w},z,\lambda,\nu)\|^3) \\ \bar{w}' = -i\bar{w} + \frac{\nu}{2}\bar{w} - z\bar{w} + O(\|(w,\bar{w},z,\lambda,\nu)\|^3) \\ z' = \lambda + z^2 + \frac{1}{2}w\bar{w} + O(\|(w,\bar{w},z,\lambda,\nu)\|^3) \end{array}\right.$$

Finally, the normal form in cartesian coordinates can be given as

$$\left\{\begin{array}{l} x' = -y + \frac{\nu}{2}x - zx + A(x,y,z,\lambda,\nu) \\ y' = x + \frac{\nu}{2}y - zy + B(x,y,z,\lambda,\nu) \\ z' = \lambda + z^2 + \frac{1}{2}(x^2+y^2) + C(x,y,z,\lambda,\nu), \end{array}\right. \tag{2.12}$$

where A, B and C are $O(\|(x,y,z,\lambda,\nu)\|^3)$ and are C^ω. Comparing with (1.2), when $\lambda = \mu = 0$, we notice that $a = 1$ and $b = 1/2$. Therefore we conclude that the extended Michelson system is an unfolding of the HZ^* singularity.

An interesting analytic one-parameter subfamily is obtained by taking $\nu = 0$. In such a case the system is volume preserving and time reversible. Both are properties which are preserved by reduction to a normal form.

3 Splitting of the invariant manifolds

3.1 Invariant manifolds in the blown-up system

For sufficiently small $\varepsilon > 0$, the vector fields (2.7) have singularities at some points $\bar{p}_\pm$, near $(0,0,1)$ and $(0,0,-1)$, respectively. The positions $\bar{p}_\pm(\varepsilon,\bar{\mu})$ depend in a C^∞ (resp.

C^ω) way on $(\varepsilon, \bar{\mu})$ for $\varepsilon \sim 0$ and $\bar{\mu} \in [-\bar{\mu}_0, \bar{\mu}_0] \subset (-a, a)$, with $\bar{p}_\pm(0, \bar{\mu}) = (0, 0, \pm 1)$. The respective 1-jets at $\bar{p}_\pm$ are

$$\begin{pmatrix} \bar{\mu} \mp a & -\frac{1}{\varepsilon} & 0 \\ \frac{1}{\varepsilon} & \bar{\mu} \mp a & 0 \\ 0 & 0 & \pm 2 \end{pmatrix} + O(\varepsilon),$$

and hence, the eigenvalues are respectively $\{\bar{\mu} - a \pm \frac{i}{\varepsilon} + O(\varepsilon), 2 + O(\varepsilon)\}$ at $\bar{p}_+$ and $\{\bar{\mu} + a \pm \frac{i}{\varepsilon} + O(\varepsilon), -2 + O(\varepsilon)\}$ at $\bar{p}_-$. Since $a > 0$ and $\bar{\mu} \in (-a, a)$, the points $\bar{p}_\pm$ are hyperbolic saddles if $\varepsilon > 0$ is sufficiently small. The equilibrium point $\bar{p}_+$ [resp. $\bar{p}_-$] has a one-dimensional unstable [resp. stable] manifold $W^u(\bar{p}_+)$ [resp. $W^s(\bar{p}_-)$] and a two-dimensional stable [resp. unstable] manifold $W^s(\bar{p}_+)$ [resp. $W^u(\bar{p}_-)$]. Depending on the regularity of the expression (2.1), these manifolds will be either C^∞ or C^ω.

Important to know is their behaviour when $\varepsilon \to 0$. This problem is not trivial because, as seen from the expression (2.7), the speed of rotation tends to infinity for $\varepsilon \to 0$ and there is no regular limiting system. There is of course a limiting system in expression (2.6) for $\varepsilon \to 0$, but unfortunately it is very degenerate representing a linear rotation around a line of singularities. It has been proved by P. Bonckaert and E. Fontich in [3] that, for $\varepsilon \to 0$, and locally near $\bar{p}_+$ [resp. $\bar{p}_-$], the one-dimensional manifold $W^u(\bar{p}_+)$ [resp. $W^s(\bar{p}_-]$ tends in a C^∞ way to the $\bar{z}$-axis. The word "local" in this statement means that the result near $\bar{p}_+$ is at least valid on a neighbourhood of the region $\{\bar{z} \geq 0\}$, while the result near $\bar{p}_-$ is at least valid on a neighbourhood of $\{\bar{z} \leq 0\}$. From the study along this section we will see that one cannot expect to improve, in general, the C^∞ character of the result in [3] to a C^ω one by working with C^ω expression (2.1).

Let us now study the behaviour of $W^s(\bar{p}_+)$ in $\{\bar{z} \geq 0\}$ when $\varepsilon \to 0$. The study of $W^u(\bar{p}_-)$ in $\{\bar{z} \leq 0\}$ will be similar. Knowing that the one-dimensional manifold $W^u(\bar{p}_+)$ extends in a C^∞ way to the $\bar{z}$-axis, we can make an $(\varepsilon, \bar{\mu})$-dependent C^∞ family of coordinate changes, translating $\bar{p}_+(\varepsilon, \bar{\mu})$ to $(0, 0, 1)$ and bringing $W^s(\bar{p}_+(\varepsilon, \bar{\mu}))$ to the $\bar{z}$-axis. The family of conjugating diffeomorphisms can be given by the cited translation followed by an expression

$$(\bar{x}, \bar{y}, \bar{z}) \quad \to \quad (\bar{x} - \varphi(\bar{z}, \varepsilon, \bar{\mu}), \bar{y} - \psi(\bar{z}, \varepsilon, \bar{\mu}), \bar{z}),$$

where $(\bar{x}, \bar{y}) = (\varphi(\bar{z}, \varepsilon, \bar{\mu}), \psi(\bar{z}, \varepsilon, \bar{\mu}))$ represents the graph of $W^u(\bar{p}_+)$ given after translation. In any case when the parameter is $(0, \bar{\mu})$, the coordinate change becomes the identity for all $\bar{\mu} \in [-\bar{\mu}_0, \bar{\mu}_0]$. As such, for the rest of this paragraph we can suppose that in expression (2.6) restricted to $\{\bar{z} \geq 0\}$, there is a singularity at $(0, 0, 1)$, while the $\bar{z}$-axis stays invariant for each $(\varepsilon, \bar{\mu})$. In these new C^∞ coordinates (2.6) can be written as

$$\left\{ \begin{array}{l} \bar{x}' = -\bar{y} + \varepsilon\bar{\mu}\bar{x} - \varepsilon a\bar{x}\bar{z} + \varepsilon^2\alpha(\bar{x}, \bar{y}, \bar{z}, \varepsilon, \bar{\mu}) \\ \bar{y}' = \bar{x} + \varepsilon\bar{\mu}\bar{y} - \varepsilon a\bar{y}\bar{z} + \varepsilon^2\beta(\bar{x}, \bar{y}, \bar{z}, \varepsilon, \bar{\mu}) \\ \bar{z}' = \varepsilon(\bar{z}^2 - 1 + b(\bar{x}^2 + \bar{y}^2)) + \varepsilon^2\gamma(\bar{x}, \bar{y}, \bar{z}, \varepsilon, \bar{\mu}), \end{array} \right. \tag{3.1}$$

with all functions C^∞, α and β are $O(\|(\bar{x}, \bar{y})\|)$, γ is $O(\|(\bar{x}, \bar{y}, \bar{z} - 1)\|$. The same of course holds for (2.7) and in particular, the corresponding system can be written as

$$\left\{ \begin{array}{l} \bar{x}' = -\frac{1}{\varepsilon}\bar{y} + \bar{\mu}\bar{x} - a\bar{x}\bar{z} + \varepsilon\alpha(\bar{x}, \bar{y}, \bar{z}, \varepsilon, \bar{\mu}) \\ \bar{y}' = \frac{1}{\varepsilon}\bar{x} + \bar{\mu}\bar{y} - a\bar{y}\bar{z} + \varepsilon\beta(\bar{x}, \bar{y}, \bar{z}, \varepsilon, \bar{\mu}) \\ \bar{z}' = \bar{z}^2 - 1 + b(\bar{x}^2 + \bar{y}^2) + \varepsilon\gamma(\bar{x}, \bar{y}, \bar{z}, \varepsilon, \bar{\mu}). \end{array} \right. \tag{3.2}$$

At least in such an expression we can introduce cylindrical coordinates around the $\bar{z}$-axis, which we will do when appropriate.

With regard to the two-dimensional invariant manifolds, we only refer to [4] where it is proved that, for $\varepsilon \to 0$ while keeping $\bar{\mu} \in [-\bar{\mu}_0, \bar{\mu}_0]$, the two-dimensional invariant manifold $W^s(\bar{p}_+))$ tends in a C^∞ way to the analytic $\bar{\mu}$-family of manifolds

$$\bar{M}_{\bar{\mu}} \;=\; \{(\bar{x}, \bar{y}, \bar{z}) \mid ((\bar{x}^2 + \bar{y}^2)^{1/2}, \bar{z}) \in M_{\bar{\mu}}\}$$

where $M_{\bar{\mu}}$ stands for the stable manifold of $Z_{\bar{\mu}}$ at $(0, 1)$ (see (2.8)). This result again holds in the entire region $\{\bar{z} \geq 0\}$.

As a first consequence of these results, we now see that for all $(\varepsilon, \bar{\mu})$ with $\varepsilon \sim 0$ and $\bar{\mu} \in [-\bar{\mu}_0, \bar{\mu}_0]$, the invariant manifolds $W^u(\bar{p}_+(\varepsilon, \bar{\mu}))$, $W^s(\bar{p}_+(\varepsilon, \bar{\mu}))$, $W^s(\bar{p}_-(\varepsilon, \bar{\mu}))$ and $W^u(\bar{p}_-(\varepsilon, \bar{\mu}))$ all intersect the plane $\{\bar{z} = 0\}$, the one-dimensional ones at a point, and the two-dimensional ones at a circle. The smoothness of the circle is C^∞ or C^ω depending on the regularity of (2.1) and tends in a C^∞ way to $\bar{M}_{\bar{\mu}_*} \cap \{\bar{z} = 0\}$ when $(\varepsilon, \bar{\mu}) \to (0, \bar{\mu}_*)$.

3.2 Trapping and the existence of Shilnikov homoclinic orbits

We consider the first intersection of the two-dimensional invariant manifolds of the equilibrium points $\bar{p}_\pm(\varepsilon, \bar{\mu}))$ of the system (2.7) and the plane $\{\bar{z} = 0\}$. More precisely, let C^u be a simple closed curve, which we simply call a circle, in the plane $\{\bar{z} = 0\}$ given by the first intersection of $W^u(\bar{p}_-(\varepsilon, \bar{\mu}))$. Similarly, let C^s be a circle in $\{\bar{z} = 0\}$ given by the first intersection of $W^s(\bar{p}_+(\varepsilon, \bar{\mu}))$. As shown in the previous subsection, these circles are well-defined as long as ε is sufficiently small. Moreover, if $|\bar{\mu}|$ is sufficiently large, depending on the sign of $\bar{\mu}$, one of the circles completely encloses the other.

Definition 3.1 If C^u lies inside C^s, we say that the system (2.7), or the corresponding parameter point, is in *forward trapping* (see Figure 2 when $\bar{\mu} < 0$), and the region in $\mathbb{R}^3$ bounded by the annulus region between C^u and C^s on the plane $\{\bar{z} = 0\}$ and the parts of the two-dimensional invariant manifolds $W^s(\bar{p}_+(\varepsilon, \bar{\mu}))$ and $W^u(\bar{p}_-(\varepsilon, \bar{\mu}))$ is called the *forward trapping region*. Similarly, if C^s lies inside C^u, the system (2.7), or the corresponding parameter point, is in *backward trapping* (see Figure 2 when $\bar{\mu} > 0$), and we define the *backward trapping region* analogously. Notice that the forward [resp. backward] trapping region, if it exists, is a positively [resp. negatively] invariant set under the flow of (2.7).

The analysis in the previous subsection shows that system (2.7) will change from forward to backward trapping by varying the parameter $\bar{\mu}$ from negative to positive, and in between, there will be a situation where circles intersect, which may lead to some dynamical consequences. Notice that if the splitting is exponentially small we should expect transversal intersections in a wedge-shaped parameter region with exponentially small width in ε.

In order to use this idea to study the existence of some homoclinic and heteroclinic orbits, we also need to study the first intersection points of the one-dimensional invariant manifolds with the plane $\{\bar{z} = 0\}$.

Definition 3.2 The set of parameters $(\varepsilon, \bar{\mu}) \neq 0$ for which the first intersection points of the one-dimensional invariant manifolds with the plane $\{\bar{z} = 0\}$ coincide is denoted by $\mathcal{E}$, and is called the *exceptional set*.

Obviously, the structure of the exceptional set provides us with crucial information about dynamics and bifurcations, in particular about the existence of Shilnikov homoclinic orbits. More specifically, considering the system (2.7) with the blow-up parameters $(\varepsilon, \bar{\mu})$, one expects that the one-dimensional invariant manifolds split at most of the parameter values in a general unfolding and hence the exceptional set, which is generically of codimension two, becomes small (and in fact it could be empty), unless (2.7) is completely rotationally symmetric, in which case, the exceptional set is the entire domain. If the unfolding is analytic, the exceptional set is an analytic set except at $\varepsilon = 0$, and hence, if one knows that the one-dimensional invariant manifolds indeed split at a parameter value, then $\mathcal{E}$ is either a set of isolated points possibly accumulating to the line $\varepsilon = 0$, or a set of analytic curves which are most likely emanating from the line $\varepsilon = 0$, in the presence of suitable symmetries.

Using the forward and backward trappings and the exceptional set, we can formulate a sufficient condition for the existence of a Shilnikov homoclinic orbit as follows:

Theorem 3.3 *Assume $0 < a < 2$ and choose $0 < \bar{\mu}_0 < \min\{a, 2-a\}$. For given $\bar{\mu}_- < 0 < \bar{\mu}_+$ with $\bar{\mu}_\pm \in [-\bar{\mu}_0, \bar{\mu}_0] \subset (-a, a)$, there exists $\varepsilon_0 > 0$ such that, if one can take a path γ in the parameter region $V = (0, \varepsilon_0] \times [\bar{\mu}_-, \bar{\mu}_+]$ that connects parameter points $(\varepsilon_\pm, \bar{\mu}_\pm)$ corresponding to forward and backward trapping, respectively, and that does not intersect the exceptional set $\mathcal{E}$, then there is a parameter point $(\varepsilon_*, \bar{\mu}_*) \in \gamma$ such that the corresponding system (2.7) possesses a Shilnikov homoclinic orbit.*

Proof. First note that we look for a Shilnikov homoclinic orbit as given by the intersection of $W^u(\bar{p}_+(\varepsilon, \bar{\mu}))$ and $W^s(\bar{p}_+(\varepsilon, \bar{\mu}))$ which passes through a neighborhood of $\bar{p}_-(\varepsilon, \bar{\mu})$. From the results explained in the previous subsection, we can choose a cylindrical neighborhood of $\bar{p}_-(\varepsilon, \bar{\mu})$ having a property that when an orbit, except one in $W^s(\bar{p}_-(\varepsilon, \bar{\mu}))$, enters the neighborhood from its top disk boundary, it exits the neighborhood from its side boundary and extends to the plane $\{\bar{z} = 0\}$. Such a neighborhood exists as long as the parameter $\bar{\mu}$ remains in a compact interval $[\bar{\mu}_-, \bar{\mu}_+]$ and for sufficiently small $\varepsilon > 0$. Let $\varepsilon_0 > 0$ be such that a cylindrical neighborhood N of $\bar{p}_-(\varepsilon, \bar{\mu})$ with the above property exists for any $(\varepsilon, \bar{\mu}) \in (0, \varepsilon_0] \times [\bar{\mu}_-, \bar{\mu}_+]$.

Now take any path $\gamma \subset (0, \varepsilon_0] \times [\bar{\mu}_-, \bar{\mu}_+]$ that does not intersect the exceptional set $\mathcal{E}$ and that connects two parameter points $(\varepsilon_\pm, \bar{\mu}_\pm)$. Along the path γ, the one-dimensional invariant manifolds of the corresponding system (2.7) must split, and hence, by choosing ε_0 smaller if necessary, we can always assure that the one-dimensional unstable manifold $W^u(\bar{p}_+(\varepsilon, \bar{\mu}))$ must enter N through its top disk boundary, and thus leaves it through its side boundary and extends to a point q in the plane $\{\bar{z} = 0\}$, which is inside the circle C^u in the plane.

At one of the boundary points of the path γ, namely $(\varepsilon_-, \bar{\mu}_-)$, the corresponding system is in forward trapping, and therefore the circle C^u lies inside C^s and any orbit that passes a point inside C^u, which includes the point q, must be confined in the forward trapping region, which is positively invariant under the flow. In particular, we see that the one-dimensional unstable manifold $W^u(\bar{p}_+(\varepsilon, \bar{\mu}))$ never intersect $W^s(\bar{p}_+(\varepsilon, \bar{\mu}))$ at the parameter $(\varepsilon_-, \bar{\mu}_-)$.

At the other boundary point $(\varepsilon_+, \bar{\mu}_+)$, on the other hand, the system is in backward trapping and the circle C^u is outside C^s, and therefore the same intersection point q is now outside the circle C^s. In order to guarantee that q is indeed outside C^s, we must notice that the splitting function of the one-dimensional invariant manifolds can be made arbitrary small by choosing ε small enough, while the distance of the circles C^u and C^s are primarily determined by $\bar{\mu}$. Therefore by making ε_0 even smaller, if necessary, we can be sure that q lies close enough to C^u and hence it is indeed outside C^s at $(\varepsilon_+, \bar{\mu}_+)$.

We have thus shown that the mutual location of q and C^s, namely, the intersection of $W^u(\bar{p}_+(\varepsilon, \bar{\mu}))$ and $W^s(\bar{p}_+(\varepsilon, \bar{\mu}))$ in the plane $\{\bar{z} = 0\}$ interchange between the two boundary points of the path γ, and hence there must exists a point in γ for which the corresponding system (2.7) has non-empty intersection of $W^u(\bar{p}_+(\varepsilon, \bar{\mu}))$ and $W^s(\bar{p}_+(\varepsilon, \bar{\mu}))$, given by the intersection of q and C^s in $\{\bar{z} = 0\}$. This shows the existence of a homoclinic orbit at the saddle-focus equilibrium point $\bar{p}_+(\varepsilon, \bar{\mu})$.

It remains to verify the Shilnikov's eigenvalue condition. From the equations (2.7), the dominant terms of the unstable eigenvalue at $\bar{p}_+(\varepsilon, \bar{\mu})$ is 2, while that of the real part of the stable eigenvalue is $\bar{\mu} - a$ which is negative and less than $-2a$. Therefore, if $0 < a < 2$ and $0 < \bar{\mu}_0 < \min\{a, 2-a\}$, we have $2 > \bar{\mu}_0 + a > |\bar{\mu} - a|$, and thus the Shilnikov's eigenvalue condition is satisfied for sufficiently small ε. This completes the proof. □

Remark 3.4 If $V \setminus \mathcal{E}$ has only one connected component then Theorem 3.3 applies.

Remark 3.5 From a result of Homburg [24], there exists a suspension of a Hénon-type strange attractor in an unfolding of the Shilnikov homoclinic orbit, provided an additional eigenvalue condition is satisfied. In the form of the equations of (2.7), this eigenvalue condition corresponds to $2(\bar{\mu} - a) + 2 < 0$. Therefore, if $a > 1$ and $0 < \bar{\mu}_0 < \min\{2 - a, a - 1\}$, then $2(\bar{\mu} - a) + 2 < 2(\bar{\mu}_0 - a + 1) < 0$ and thus this eigenvalue condition is satisfied as well as the Shilnikov's eigenvalue condition. If $a \leq 1$, on the other hand, we need to know a more precise information on the parameter value $\bar{\mu}_*$ at which the Shilnikov homoclinic orbit occurs and this may not be easy to obtain by the method given here.

3.3 Accumulation of the Bykov cycles in a reversible unfolding

In this subsection, bearing in mind the Michelson system (1.7), we consider the class of reversible unfoldings. Namely, we assume that an involution of the form

$$(\bar{x}, \bar{y}, \bar{z}, t) \mapsto (-\bar{x}, \bar{y}, -\bar{z}, -t)$$

leaves the system (2.7) invariant. In particular, we must set $\bar{\mu} = 0$. Observe that the vector fields that appear in the above unfolding satisfy the following properties:

(R1) The $\bar{y}$-axis is the fixed point set of the reversibility involution.

(R2) There are two saddle foci $\bar{p}_\pm$ which do not lie on the fixed point set of the involution, and which are related by the involution.

(R3) The unstable manifold of $\bar{p}_+$ is one-dimensional and its stable manifold is two-dimensional. (Therefore it follows from (R2) that the stable [resp. unstable] manifold of $\bar{p}_-$ is one-dimensional [resp. two-dimensional].)

Note that we can consider a reversible unfolding of a Hopf-zero singularity in a more general context, for which the reversible involution needs not to be of the above form. However, assuming that the reversible involution is linear, and that the fixed point set of the involution is one-dimensional and does not contain the equilibria bifurcating from the Hopf-zero singularity, it is possible to bring the system into the above form by a suitable coordinate change, and therefore we study (2.7) under the above reversibility without losing generality.

Let $\mathfrak{X}_R$ be the set of all vector fields on $\mathbb{R}^3$ which are reversible under the above involution and which satisfy the properties (R1)-(R3). In this class of vector fields, one can discuss an important invariant set called the Bykov cycle. Below, we shall give a definition of the Bykov cycle only for a reversible vector field in $\mathfrak{X}_R$, but it can also be considered for a larger class of vector fields which are not necessarily reversible. The goal of this subsection is to prove the existence and accumulation of the Bykov cycles to the Hopf-zero singularity.

Definition 3.6 For a vector field $X \in \mathfrak{X}_R$, a *Bykov cycle* is a heteroclinic cycle consisting of an intersection of the one-dimensional invariant manifolds $W^u(\bar{p}_+)$ and $W^s(\bar{p}_-)$, together with a transverse intersection of the two-dimensional invariant manifolds $W^u(\bar{p}_-)$ and $W^s(\bar{p}_+)$.

Observe that, because of the reversibility, the one-dimensional invariant manifolds $W^u(\bar{p}_+)$ and $W^s(\bar{p}_-)$ are related by the involution. In particular, if one of them intersects the fixed point set of the involution, then the other must do at the same point, and hence the existence of a one-dimensional connection is equivalent to the existence of intersection between the fixed point set of involution and $W^u(\bar{p}_+)$ (or $W^s(\bar{p}_-)$). This remark helps the bifurcation analysis of the Bykov cycle in reversible vector fields.

Theorem 3.7 *Consider an ε-family of reversible vector fields of the form (2.7) with $\bar{\mu} = 0$ which belong to $\mathfrak{X}_R$. Assume, for sufficiently small $\varepsilon > 0$, that the exceptional set $\mathcal{E}$ is empty and that the two-dimensional invariant manifolds $W^u(\bar{p}_-(\varepsilon))$ and $W^s(\bar{p}_+(\varepsilon))$ do split and have a non-empty transverse intersection.*

Then there is a sequence $\{\varepsilon_n\}$ converging to $\varepsilon = 0$ such that the corresponding vector fields have a Bykov cycle.

Proof. We first remark that the vector field with sufficiently small $\varepsilon > 0$ has a cylindrical neighborhood near $\bar{p}_-(\varepsilon)$ satisfying the property used in the proof of Theorem 3.3. Within this range of small $\varepsilon > 0$, consider the one-dimensional manifold $W^u(\bar{p}_+)$ which enters the neighborhood from the top disk boundary and exits from its side boundary because the exceptional set is empty for sufficiently small $\varepsilon > 0$. Using the result of [3] again, we know that it then hits the plane $\{\bar{z} = 0\}$ at a point $\bar{q} = \bar{q}(\varepsilon)$. Since there is a rotation in the cylindrical neighborhood and since the splitting function of the one-dimensional invariant manifolds measured on the top disk boundary of the neighborhood shrinks to 0 as $\varepsilon \to 0$, the intersection point $\bar{q}(\varepsilon)$ rotates in the plane $\{\bar{z} = 0\}$ and accumulates to C^u, the circle introduced in the previous subsections.

Note that the circle itself also depends on ε and rotates as ε varies, but it always encloses the origin of the plane $\{\bar{z} = 0\}$, and hence it always cuts the $\bar{y}$-axis, the fixed point set of the involution. Note also that, the smaller the parameter ε becomes, the faster the point $\bar{q}(\varepsilon)$ rotates along the circle C^u, as the imaginary part of the eigenvalue at the equilibrium point $\bar{p}_-(\varepsilon)$ is given principally by $1/\varepsilon$. Therefore as $\varepsilon \to +0$ the point $\bar{q}(\varepsilon)$ intersects the $\bar{y}$-axis infinitely many times at $\varepsilon = \varepsilon_n (\to 0)$, and at each intersection, it crosses the line at a non-zero speed as ε is varied, at least for sufficiently small ε.

Recalling that the intersection of $W^u(\bar{p}_+(\varepsilon))$ and the fixed point set of the involution implies the non-empty intersection of the one-dimensional invariant manifolds $W^u(\bar{p}_+(\varepsilon))$ and $W^s(\bar{p}_-(\varepsilon))$, we have shown the existence of a Bykov cycle, because the transverse intersection of the two-dimensional manifold is taken as an assumption. Thus this completes the proof of the existence and accumulation of the Bykov cycles to the Hopf-zero singularity. □

Remark 3.8 In [33], J. Lamb, M. A. Teixeira, and K. Webster have shown the accumulation of the Bykov cycles to the *HZ** singularity in its reversible generic unfoldings, as well as a number of dynamical consequences from it. The genericity is for the C^∞-topology on a neighborhood of the origin in $\mathbb{R}^3 \times \mathbb{R}$. Their argument is to construct a flat perturbation of a rotationally symmetric unfolding of the *HZ** singularity in a way that it contains a sequence of parameter values at which the Bykov cycle occurs. In a similar way one obtains a sequence of parameter values at which a Shilnikov homoclinic orbit occurs. The flat perturbation (see §4 of [33]) is such that it enables to control the splitting of the one-dimensional and two dimensional invariant manifolds in a suitable way; it uses essentially the same geometric mechanisms for the creation of such homoclinic and heteroclinic orbits as we use in this and later sections of this paper. However, their results, though generic in the C^∞-topology, cannot be directly applied to a given specific unfolding. We want to emphasize the exact role that the splitting of these invariant manifolds and the splitting functions play in the study of the dynamics of individual unfoldings of the *HZ** singularity. We therefore formulate our results in terms of the splitting properties of these manifolds, hoping to be able to apply the results to any concrete system of which the splitting functions satisfy the assumptions that we make in our theorems. See also §3.6. Note also that Lamb et al. [33] gave some results of bifurcations around the *HZ** singularity in the Michelson system by using information of the splitting of these invariant manifolds.

We finally remark that the assumptions of the theorem may be weakened for an analytic reversible unfolding. In fact, if the unfolding is analytic then, once we know that the two-dimensional invariant manifolds do split, there will be an intersection that is either transverse or of odd (finite) order contact, and hence it is always topologically transverse. Moreover, by an argument used in [33], one may be able to show that, when they intersect at an odd order contact, they also have a transverse intersection at a different place, so that the two-dimensional invariant manifolds always have a transverse intersection.

3.4 Splitting functions

Removing terms of order $O(\varepsilon)$ in (3.2) we get:

$$\begin{cases} \bar{x}' = -\frac{1}{\varepsilon}\bar{y} + \bar{\mu}\bar{x} - a\bar{x}\bar{z} \\ \bar{y}' = \frac{1}{\varepsilon}\bar{x} + \bar{\mu}\bar{y} - a\bar{y}\bar{z} \\ \bar{z}' = \bar{z}^2 - 1 + b(\bar{x}^2 + \bar{y}^2). \end{cases} \tag{3.3}$$

It should be noticed that the above system is conservative for $\bar{\mu} = 0$ and reversible under the involution $R : (\bar{x}, \bar{y}, \bar{z}) \to (-\bar{x}, \bar{y}, -\bar{z})$ and the time reverse $t \to -t$.

As already mentioned, taking cylindrical coordinates in the above expression and forgetting the rotational component we get, for $\bar{\mu} = 0$,

$$\left\{ \begin{array}{l} \bar{r}' = -a\bar{r}\bar{z} \\ \bar{z}' = -1 + \bar{z}^2 + b\bar{r}^2, \end{array} \right. \tag{3.4}$$

having the first integral $H = \bar{r}^{2/a}[1-\bar{z}^2-b\bar{r}^2/(a+1)]$. Note that in general the integrability is destroyed by the terms of order $O(\varepsilon)$. The $\bar{z}$ component along the two heteroclinic connections corresponding to $H = 0$ is given by

$$\begin{array}{rclll} \bar{z}(t) & = & \tanh(-t) & \text{for} & \bar{r} = 0, \quad \text{or} \\ \bar{z}(t) & = & \tanh(at) & \text{for} & \bar{z}^2 + b\bar{r}^2/(a+1) = 1. \end{array}$$

It was proved in Section §3.1 that, for family (3.2), the one-dimensional and the two-dimensional invariant manifolds, all cut the plane $\bar{z} = 0$. They do it at points and simple closed curves respectively. The intersection points of the one-dimensional invariant manifolds depend in a C^∞ way on the parameters and tend to $(\bar{x}, \bar{y}) = (0, 0)$ as $(\bar{\mu}, \varepsilon) \to (0, 0)$. In the sequel $S^{(1)}(\bar{\mu}, \varepsilon)$ will denote the splitting function between the intersection points. On the other hand the simple closed curves given by the intersection of the two-dimensional invariant manifolds move also in a C^∞ way with respect to the parameters and tend to the circle $\bar{x}^2 + \bar{y}^2 = (1 + a)/b$ as $(\bar{\mu}, \varepsilon) \to (0, 0)$. We will denote by $S^{(2)}(\varphi, \bar{\mu}, \varepsilon)$ the radial splitting function between the curves. Note that both splittings are functions of $\bar{\mu}$ and ε but $S^{(2)}$ also depends on an angular variable φ. When $\varepsilon \neq 0$, $S^{(1)}$ and $S^{(2)}$ are C^∞ or C^ω if the family is C^∞ or C^ω, respectively. Nevertheless they are only C^∞ at $\{\varepsilon = 0\}$ even if the family is C^ω.

Two different kind of contributions to the splitting functions need to be taken into account. Terms preserving the rotational symmetry have no effect on $S^{(1)}$ since they leave the vertical axis invariant. On $S^{(2)}$ their contribution has leading terms of finite order in $\bar{\mu}$ and ε and the classical Melnikov analysis can be used. The leading term in $\bar{\mu}$ is of order 1 and it is affected by a non zero coefficient which is determined by the integral of r along the heteroclinic orbit of system (3.4) on $z^2 + br^2/(a + 1) = 1$. We could generically assume that the leading term in ε is of order 1 but we will not need it in this paper. The coefficient, obtained by evaluation of the appropriate integrals along the heteroclinic orbit, only depends on the third order terms in the normal form of the singularity preserving the rotational symmetry.

On the other hand the contribution to both $S^{(1)}$ and $S^{(2)}$ of the terms which break the rotational symmetry tends to 0 beyond all orders in ε since they can be removed from the normal form up to any arbitrarily high order.

In the sequel we will write

$$S^{(2)}(\varphi, \bar{\mu}, \varepsilon) = S^{(2)}_{\mathrm{f}}(\bar{\mu}, \varepsilon) + S^{(2)}_{\mathrm{b}}(\varphi, \bar{\mu}, \varepsilon)$$

where $S^{(2)}_{\mathrm{f}}$ is a C^∞ or C^ω function, depending on the regularity of the family, and is only determined by the rotationally symmetric part of the family. The function $S^{(2)}_{\mathrm{b}}$ is the remainder term and it is C^∞ or C^ω when $\varepsilon \neq 0$, depending on the regularity of the family, but only C^∞ at $\varepsilon = 0$, even if the family is C^ω. Note that, as explained above,

$$S_{\mathrm{f}}^{(2)}(\bar{\mu}, \varepsilon) = \alpha_1 \bar{\mu} + \alpha_2 \varepsilon + o(\|(\bar{\mu}, \varepsilon)\|)$$

with $\alpha_1 \neq 0$ and

$$S_{\mathrm{b}}^{(2)}(\varphi, \bar{\mu}, \varepsilon)/|\varepsilon|^m \to 0$$

as $\varepsilon \to 0$ uniformly in φ and $\bar{\mu}$ for all $m \in \mathbb{N}$.

It follows from [2] that $\|S^{(1)}(\bar{\mu}, \varepsilon)\|$ is exponentially small with respect to the parameter ε and we can assume as a generic condition that

$$\|S^{(1)}(\bar{\mu}, \varepsilon)\| \leq C_1 \varepsilon^{-(1+a)} \exp\left(-\frac{\pi}{2\varepsilon}\right) \tag{3.5}$$

for some constant $C_1 > 0$. Moreover we conjecture that $\|S_{\mathrm{b}}^{(2)}(\varphi, \bar{\mu}, \varepsilon)\|$ is also exponentially small with respect to ε and

$$\|S_{\mathrm{b}}^{(2)}(\varphi, \bar{\mu}, \varepsilon)\| \leq C_2 \varepsilon^{N_2} \exp\left(-\frac{\pi}{2a\varepsilon}\right)$$

for some constants $C_2 > 0$, $N_2 \in \mathbb{R}$.

Remark 3.9 In fact, applying the formula provided in [2] to system (2.1), it follows that the leading term for the splitting distance between the one-dimensional invariant manifolds is given by

$$C_1 |\lambda|^{-a/2} \exp\left(-\frac{\pi}{2|\lambda|^{1/2}}\right),$$

for some positive constant C_1. Taking into account that, as given in (2.3), $|\lambda| = \varepsilon^2$, and also the scaling in (2.5), we get (3.5).

Let us give a sketch concerning the splitting of the 2D manifolds. Here we assume that we are either in a conservative case (zero divergence) or that there exists some reversibility forcing the existence of heteroclinic intersections between the 2D manifolds.

We can fix a meridian halfplane and consider the Poincaré map with respect to it. It is well defined near $H = 0$ for $r > 0$ except on a vicinity of the poles. Near the poles one can define the Poincaré map *around the 1D manifold*. Of course, it is not defined on the 1D manifold itself but can be extended to it by continuity. Let us denote that map as $\mathcal{P}_\varepsilon$.

In that way, for the limit flow, one has a heteroclinic connection between two hyperbolic fixed points. That manifold can be parametrized by t, so that when $t \to -\infty$ the points tend to the south pole and when $t \to +\infty$ the points tend to the north pole. As mentioned before the expression of the vertical coordinate along that connection is $\bar{z}(t) = \tanh(at)$. It can be extended to a complex strip around the real axis provided the imaginary part satisfies $|\mathrm{Im}(t)| < \pi/(2a)$, to avoid singularities. Of course, the same is true for the Poincaré map $\mathcal{P}_\varepsilon$ associated to the flow, close to the time $2\pi\varepsilon$-map of the flow. The Poincaré map $\mathcal{P}_\varepsilon$ is ε^2 close to $\mathcal{P}_0$.

Following the methodology introduced in [17, 18] one can parametrize in a suitable way the 1D manifolds of the upper and lower hyperbolic fixed points of the Poincaré map, to be denoted as N and S, respectively. As usual one can introduce a parametrization of the unstable manifold $W^u(S)$ (for the Poincaré map) of S as $g(\sigma)$ such that $\mathcal{P}_\varepsilon(g(\sigma)) = g(\lambda(\varepsilon)\sigma)$ where $\lambda(\varepsilon)$ is the dominant eigenvalue of $D\mathcal{P}_\varepsilon(\mathcal{S})$, of the form $1+O(\varepsilon)$. Then we introduce a new parameter $\tau = \log(\sigma)$. Denoting by G the parametrization in τ one has $\mathcal{P}_\varepsilon(G(\tau)) = G(\tau + h(\varepsilon))$, where $h(\varepsilon) = \log(\lambda(\varepsilon))$. The parameter τ is close to the time used for the flow. Hence $W^u(S)$ can be extended to a domain such that the imaginary part of the parameter τ is, in absolute value, bounded away from $\pi/(2a)$.

As it follows from Birkhoff Normal Form, there exists a local function H_ε, to be denoted as *energy* around S which is preserved under the action of $\mathcal{P}_\varepsilon$. It can be extended by iteration along $W^u(S)$, and it is $h(\varepsilon)$-periodic by construction. This new energy is an $O(\varepsilon)$ perturbation of the energy H. One can select H_ε such that it is zero on $W^u(S)$.

Around N we can do a similar construction for $W^s(N)$, the stable manifold (for the Poincaré map) of N. The parametrization by a parameter, say, $\hat{\tau}$ is close again to the manifold of the limit flow and, therefore to $W^u(S)$. As before the parametrization of $W^s(N)$ is $\hat{h}(\varepsilon)$-periodic in $\hat{\tau}$. The difference between $\hat{h}(\varepsilon)$ and $h(\varepsilon)$ is irrelevant and can be cancelled by a linear rescaling of $\hat{\tau}$, close to the identity. We can *measure the distance* between $W^u(S)$ and $W^s(N)$ by computing H_ε along $W^s(N)$. This gives a function, say ΔH_ε, which is $h(\varepsilon)$-periodic in τ.

To compute the harmonics of ΔH_ε one can replace a path going from τ^* to $\tau^* + h(\varepsilon)$ by one going from $\tau^* \pm \mathrm{i}K$ to $\tau^* + h(\varepsilon) \pm \mathrm{i}K$, where τ^* is any value of the parameter τ and K a positive constant bounded away from $\pi/(2a)$. The independent term is bounded by the fact that there exist heteroclinic points. This gives immediately the exponentially small bounds. Furthermore, the first harmonic will be generically the dominant one, the exponentially small term affecting the k-th harmonic being of the order of the k-th power of the exponentially small term of the first one.

The *oscillation* of $W^s(N)$ with respect to $W^u(S)$ for $\mathcal{P}_\varepsilon$ transfers immediately to a difference between the intersections of the 2D manifolds of S and N, under the perturbed flow, with the $\bar{z} = 0$ plane.

The effect of additional terms like a coefficient $\bar{\mu}$ in (3.3) is to shift one manifold with respect to the other by an amount which is, generically, $O(\bar{\mu})$. Also the consideration of systems obtained by perturbation of (3.3) with $\bar{\mu} = 0$ but $a \neq 1$, can give a shift of one manifold with respect to the other by an amount $O(\varepsilon^k)$ for some $k > 0$ if the system is not reversible.

In what follows we will provide several numerical experiments supporting the fact that $S^{(1)}(\bar{\mu}, \varepsilon)$ and $S_{\mathrm{b}}^{(2)}(\varphi, \bar{\mu}, \varepsilon)$ are exponentially small in ε. With the exception of the analysis of the extended Michelson system (1.6), which will be considered in the next subsection, all the tests below have been made by adding a new term to the first component in (3.3) (with $\bar{\mu} = 0$) after multiplying the family by a factor ε to avoid working with a rotation speed tending to ∞ as $\varepsilon \to 0$.

Test 1 Adding $\varepsilon^2 \bar{x}\bar{y}\bar{z}$:

Note that the perturbed system is still time-reversible under the involution R but not conservative. Of course, the perturbation leaves the connection along the one-dimensional invariant manifolds unchanged and hence $S^{(1)} = 0$. Concerning $S^{(2)}$ we have computed the first intersection of $W^u(S))$ with $\bar{z} = 0$. This manifold and $W^s(N)$ intersect with $\varphi = \pi/2, 3\pi/2$. Further intersections can occur when ε is large, but for small ε only these two R-invariant heteroclinic connections are present.

After several experiments with different values of a, b, ε the following formula seems to be correct

$$S_{\mathrm{b}}^{(2)} = \exp\left(-\frac{\pi}{2a\varepsilon}\right) \varepsilon^{-(2+\frac{2}{a})} A^{(2)}(a, b, \varepsilon) \cos\varphi,$$

where $A^{(2)}(a, b, \varepsilon)$ tends to a constant when $\varepsilon \to 0$. This constant seems to be proportional to $a^{-2}b^{-1}$.

Test 2 Adding $\varepsilon^2 \bar{z}^3$:

It is clear that to produce both, one- and two-dimensional, splittings, the first (or the second) equation in (3.3) must be perturbed by adding at least one term which depends only on $\bar{z}$. Otherwise the connection along the one dimensional invariant manifolds is preserved. We tried by adding a term $\varepsilon^2 \bar{z}^3$. Note that the perturbed system is no longer time-reversible with the reversor R, but it is reversible with the respect to the change $(t, \bar{x}, \bar{y}, \bar{z}) \leftrightarrow (-t, \bar{x}, -\bar{y}, -\bar{z})$. Furthermore, it is non conservative unless $a = 1$. Moreover there is an added difficulty, because the fixed points are not preserved. They are of the form $(O(\varepsilon^3), O(\varepsilon^2), \pm(1 - O(\varepsilon^4)))$. The values of the splittings are

$$\|S^{(1)}\| = \exp\left(-\frac{\pi}{2\varepsilon}\right) \varepsilon^{-(1+a)} A^{(1)}(a, b, \varepsilon),$$

$$S_{\mathrm{b}}^{(2)} = \exp\left(-\frac{\pi}{2a\varepsilon}\right) \varepsilon^{-(2+\frac{2}{a})} A^{(2)}(a, b, \varepsilon) F(\varphi).$$

with F periodic. The coefficients $A^{(1)}, A^{(2)}$ also tend to limits when $\varepsilon \to 0$. The limits seem to be essentially independent of b. We have not found a simple fit for the behaviour of the limits as a function of a.

Test 3 Adding $\varepsilon^2(\bar{z}^3 - \bar{z})$:

The system has the same reversibility as in the case of Test 2. With this perturbation the fixed points remain at the same place, paying the price of adding a small linear term. The interesting fact is that, except for the value of $A^{(1)}, A^{(2)}$, nothing changes with respect to the case of Test 2. Notice that it can happen that when the values of a, b vary, the infinitely many values of ε, where, according to the theoretical results, there is a homoclinic orbit, approach zero. We have done many tests to look for homoclinic connections and everything runs as predicted, but the values of ε where connections start to appear go to zero as $a \to \infty$ (taking $b = 1/2$ fixed). For instance, while for $a = 1$ it seems that the condition is satisfied for ε as large as 0.5, when $a = 2$ it holds for $\varepsilon < 0.2632$ (and, correspondingly, connections appear from that value of ε on, going down to 0). For $a = 4$ it holds for $\varepsilon < 0.0839$, for $a = 8$ it holds for $\varepsilon < 0.0314$, etc.

Test 4 The next set of experiments aims at making possible the destruction of the reversibility. To this end we consider the following system

$$\begin{aligned}
\bar{x}' &= -\bar{y} - \varepsilon a \bar{x}\bar{z} + \varepsilon^2(\bar{z}^3 + \alpha_1 \bar{y}^2 \bar{z} + \alpha_2 \bar{y}\bar{z}^2), \\
\bar{y}' &= \bar{x} - \varepsilon a \bar{y}\bar{z} + \varepsilon^2(\bar{z}^3 + \beta_1 \bar{x}^2 \bar{z}), \\
\bar{z}' &= \varepsilon(\bar{z}^2 - 1 + b(\bar{x}^2 + \bar{y}^2)).
\end{aligned}$$

It is clear that if $\alpha_1 = \beta_1, \alpha_2 = 0$ the system is reversible with respect to $(t, \bar{x}, \bar{y}, \bar{z}) \leftrightarrow (-t, \bar{y}, \bar{x}, -\bar{z})$. Furthermore, if $a \neq 1$ the divergence is nonzero, while for $a = 1$ the system is divergence-free for all values of α_1, α_2 and β_1. Many values of ε have been checked for different sets of $(a, b, \alpha_1, \alpha_2, \beta_1)$. Typically we start with values of ε around 0.3 or 0.2 and decrease them until we reach values like 0.05 or smaller, stopping computations when the minima of the splittings are of the order of 10^{-14}. We can summarize part of the results as follows.

a) For $a \neq 1$ and either $\alpha_1 \neq \beta_1$ or $\alpha_2 \neq 0$ the system is neither reversible nor conservative. For large ε like 0.3 or 0.2 there are still transversal heteroclinic intersections of the 2D manifolds. For smaller values of ε there is a heteroclinic tangency and the heteroclinic points disappear. For $\varepsilon \to 0$ the distance between manifolds on $\bar{z} = 0$ is $O(\varepsilon^5)$. One has to introduce a suitable $\bar{\mu}(\varepsilon)$ to recover heteroclinic phenomena.

b) In case $\alpha_1 = \beta_1, \alpha_2 = 0$ the system is reversible as said before. The 1D and 2D splitting behave as in case of Test 2 but the function F, describing the *shape* of the splitting, also depends on ε. Either if the system is conservative or not, heteroclinic intersections appear with arguments $\pi/4$ and $5\pi/4$. It can happen that additional heteroclinic intersections show up for some range of ε. For instance, for $(a, b, \alpha_1, \alpha_2, \beta_1) = (2, 1, 1, 0, 1)$ two additional heteroclinic points appear for $\varepsilon \approx 0.075386798$ and disappear for $\varepsilon \approx 0.075385636$ by means of cubic tangencies. Locally in ε the evolution of the (signed) distance between the 2D manifolds on $z = 0$ behaves like the function $M \sin(\varphi) + \sin(2\varphi)$ when M moves from $M \gg 1$ to $M \ll -1$.

c) Finally we have considered conservative ($a = 1$) non-reversible cases. In all cases the 1D and 2D splitting behave as in case of Test 2 but, as in b), the function F depends also on ε. It has also been found that there are exactly two heteroclinic points for small ε. The difference of its arguments tends to π as ε^m for some $m > 1$. Some features found in the numerical experiments are

   i) A couple of heteroclinic points, say (h_1, h_2), exist for large ε and at some ε^* a new couple (h_3, h_4) is created. Later on, for some $\varepsilon^{**} < \varepsilon^*$ the points h_1, h_2 merge in a tangency while h_3, h_4 seem to keep existing for $\varepsilon < \varepsilon^{**}$. An example of this type occurs for $(a, b, \alpha_1, \alpha_2, \beta_1) = (1, 2, 1, 2, 1)$.

   ii) For the full range of ε explored there are two heteroclinic points on $\bar{z} = 0$. The difference of arguments, say $\zeta_i(\varepsilon), i = 1, 2$, is close to π. But there is a range in which the arguments change quickly, with derivatives of the argument with respect to ε which reach a value $d\zeta_i(\varepsilon)/d\varepsilon$ near -348. An example of this type is found for $(a, b, \alpha_1, \alpha_2, \beta_1) = (1, 1, 1, 1, 1)$ and the given value, which is the maximal one in absolute value, is obtained for $\varepsilon \approx 0.18269$.

On the other hand we can consider the intersection of the unstable manifold of the upper fixed point, N, with $\bar{z} = 0$ when going up for the first time. That is, after passing close to S. This concerns not only the cases presented in Test 4, but also in the previous items. For fixed parameters of the vector field, let $\chi(\varepsilon)$ be the argument of that intersection. In all cases it has been checked that $\chi(\varepsilon) = M\varepsilon^2 + o(\varepsilon^2)$, being M a positive constant.

This is in agreement with the theoretical expectations. Using cylindrical coordinates near S, say $\hat{r}, \hat{z}$, consider the passage from a point in $\hat{z} = \Gamma$ to $\hat{r} = \Gamma$ for a small but fixed value of Γ and ε small enough. Assume that the initial point has $\hat{r} = \hat{r}_0 = A\varepsilon^B \exp(-C/\varepsilon)$ for suitable A, B, C constants, $A, C > 0$. The flying time until $\hat{r} = \Gamma$ has a dominant term of the form $t = \log(\Gamma/\hat{r}_0)/(a\varepsilon) = C/(a\varepsilon^2) + O((\log(\varepsilon))/\varepsilon)$. This gives a value of the argument on the point along the manifold whose dominant part is $2\pi C/(a\varepsilon^2)$.

In particular it has been checked that in the case mentioned in item ii) above, for $(a, b, \alpha_1, \alpha_2, \beta_1) = (1, 1, 1, 1, 1)$ and $\varepsilon \approx 0.18269$ one has $d\chi(\varepsilon)/d\varepsilon \approx -414$. That is, even in this highly exceptional case one has $|d\zeta_i(\varepsilon)/d\varepsilon| < |d\chi(\varepsilon)/d\varepsilon|$.

Several remarks related to the above experiments will be made after we have stated Theorem 3.12.

The results in these experiments show that the dominant parts of the splitting (i.e., the exponentially small terms) are of the order of what can be obtained as an a priori upper bound by considering the related manifolds for complex time.

3.5 Splitting functions in the extended Michelson system

We have done some numerical experiments with the family

$$\begin{aligned} \dot{X} &= Y \\ \dot{Y} &= Z \\ \dot{Z} &= -1 + \alpha Y + \beta Z + X^2 \end{aligned} \tag{3.6}$$

with $\dot{} = d/d\tau$, $\alpha \in (-\infty, 0)$ and $\beta \in \mathbb{R}$, which is equivalent to (1.6), when $\lambda < 0$, by means of:

$$x = \varepsilon^3 X, \quad y = \varepsilon^4 Y, \quad z = \varepsilon^5 Z, \quad \tau = \varepsilon t, \quad \lambda = -\varepsilon^6, \quad \nu = \varepsilon\beta, \quad \alpha = -\varepsilon^{-2}.$$

Note that in the above family, the Hopf-Zero singularity is found at the limit when $\beta = 0$ and $\alpha \to -\infty$.

In family (3.6) the equilibrium points are given as $Q_\pm = (\pm 1, 0, 0)$. We are interested in the behaviour of the splitting of the one- and two-dimensional invariant manifolds as $\alpha \to -\infty$ in both conservative ($\beta = 0$) and non-conservative ($\beta \neq 0$) cases.

First we consider the splitting of the one-dimensional invariant manifolds in the conservative case. It is computed from analytic approximations to the one-dimensional invariant manifold of Q_-, expressed as the graph of functions $Y = f_1(X)$ and $Z = f_2(X)$ whose coefficients are computed recurrently up to order 50. Taking into account the reversibility of (3.6), it follows that, if the first intersection of $W^u(Q_+)$ with $X = 0$ occurs at $(Y^*(\alpha), Z^*(\alpha))$ then the first intersection of $W^s(Q_-)$ with $X = 0$ occurs at $(Y^*(\alpha), -Z^*(\alpha))$. Then the splitting is in the Z direction and it can be given as $||S^{(1)}(\alpha)|| = 2|Z^*(\alpha, \beta)|$. In Figure 3, Z^* is shown for values of α ranging from -2 to -14

with stepsize -0.02. It is checked that an excellent fit for $Z^*(\alpha)$ on the range $[-14,-8]$ is given by

$$Z^*(\alpha) = -\frac{\pi}{4}|\alpha|^4 \exp\left(-\frac{\pi}{2}|\alpha|^{3/2}\right). \tag{3.7}$$

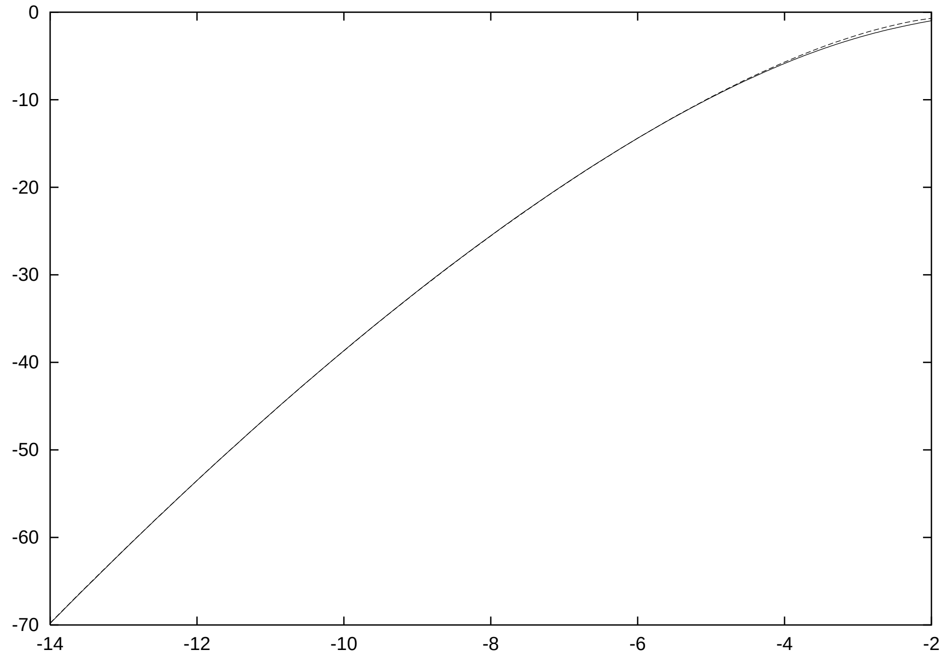

Figure 3: The one-dimensional splitting of the extended Michelson system for the conservative case. On the horizontal axis we plot the variable α, while on the vertical axis we display $\ln(-Z^*(\alpha))$ as a solid line. The dashed line is a plot of the graph of (3.7). Only for small values of $|\alpha|$ one can see a discrepancy.

We now turn to the case $\beta \neq 0$. It is again enough to study $W^u(Q_+)$. Indeed, if the intersection with $X=0$ of $W^u(Q_+)$ occurs at $(Y^*(\alpha,\beta), Z^*(\alpha,\beta))$ then the splitting vector is given by

$$S^{(1)}(\alpha,\beta) = (S_Y^{(1)}(\alpha,\beta), S_Z^{(1)}(\alpha,\beta)) = (Y^*(\alpha,\beta) - Y^*(\alpha,-\beta), Z^*(\alpha,\beta) + Z^*(\alpha,-\beta)).$$

It has been observed that for a fixed value of β the splitting vector $S^{(1)}$ spirals around $(0,0)$ as $\alpha \to \infty$. But the spires do not look like circles with decreasing radius, because the value of $S_Y^{(1)}$ seems to have an additional scaling by a factor $1/\sqrt{\alpha}$ when we compare it with $S_Z^{(1)}$. This suggest to take as radius of the splitting the quantity Δ given by

$$\Delta(\alpha,\beta) = \left(|\alpha|(S_Y^{(1)}(\alpha,\beta))^2 + (S_Z^{(1)}(\alpha,\beta)))^2\right)^{1/2}.$$

Furthermore, it is suitable to plot $\log(\Delta)$ and, taking into account the study in the conservative case (see (3.7) where the exponential term contains a factor $|\alpha|^{3/2}$), to raise this logarithm to the power $2/3$ in order to have a smoother behaviour.

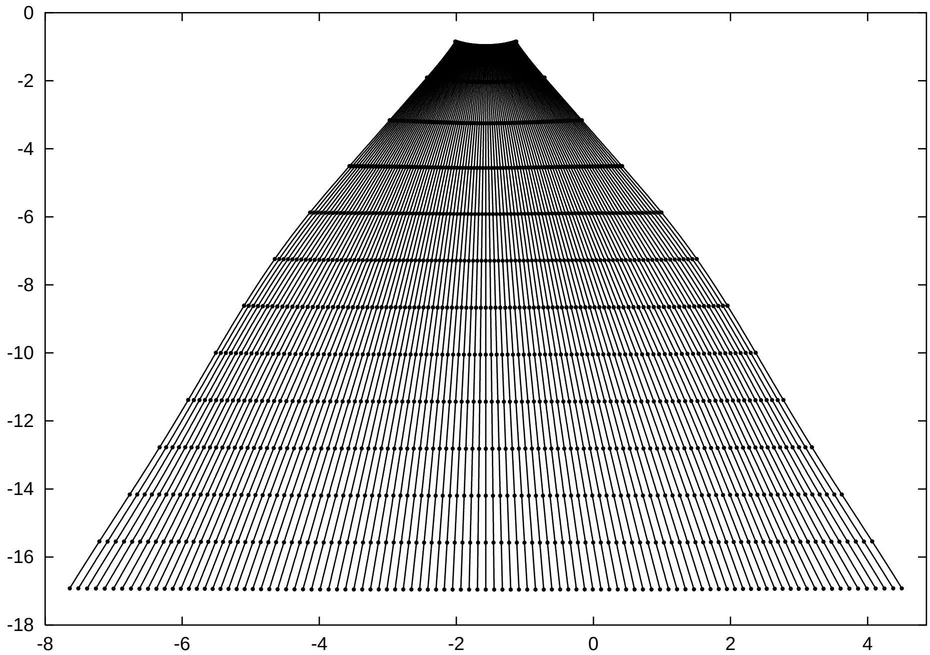

Figure 4: The one-dimensional splitting of the extended Michelson system in the dissipative case. On the horizontal axis we plot the argument of the vector splitting $S^{(1)}$ whereas in the vertical axis $(\log(\Delta))^{2/3}$ is plotted. Solid lines from right to left correspond to constant values of β which range from -0.5 to 0.5 with a stepsize 0.01. The values corresponding to α integer are marked with points. They correspond to $\alpha = -14$ on the bottom and $\alpha = -2$ on the top.

Concerning the angle, we simply compute the argument of the vector $S^{(1)}$ using the appropriate determination to have continuous functions of α for fixed values of β. Both, $(\log(\Delta))^{3/2}$ and the splitting argument are shown in Figure 4.

To study the splitting of the two-dimensional invariant manifolds it is enough, due to the reversibility, to compute $W^u(Q_-)$ as a function of α in the conservative case and to compute it for (α, β) and $(\alpha, -\beta)$ in the general case. Indeed, $W^s(Q_+)$ at (α, β) is obtained as the image of $W^u(Q_-)$ at $(\alpha, -\beta)$ by the map $(X, Y, Z) \to (-X, Y, -Z)$. Since the flow spirals up and down with respect to the X variable when it goes up close to $W^u(Q_-)$, it is better to consider a section different from $X = 0$. The idea is to get a surface Σ such that the curve determined by the first intersection of $W^u(Q_-)$ with Σ is a closed curve. To this end the original extended Michelson system (1.6) is written in normal form up to second order (see (2.12)). The section $z = 0$ in the normal form variables is taken as a suitable section. With respect to variables (X, Y, Z), Σ can expressed as $\Sigma = \{(X, Y, Z) \in \mathbb{R}^3 \,|\, g(X, Y, Z) = 0\}$ where

$$g(X, Y, Z) = |\alpha|^4 X + (|\alpha|^3 - 2)Z + (|\alpha|Y - 1)(|\alpha|^2\beta + 2|\alpha|X + 3Z/2). \tag{3.8}$$

Note that Σ is invariant under the involution.

We only consider the conservative case. On $W^u(Q_-)$ the variable Z is expressed as the the graph of a function in (X, Y) and such function is computed up to order

50. From this a curve on $W^u(Q_-)$ diffeomorphic to $\mathbb{S}^1$ at a distance of the order of a fraction of the unity from Q_- is computed for a sample of initial angles. Then the flow is integrated numerically, using a high order Taylor method, until the first intersection with Σ is reached. Let $(Y(\varphi_i), Z(\varphi_i))$ be the coordinates in Σ with respect to an initial angle φ_i. Coordinates $Y(\varphi_i)$ and $Z(\varphi_i)$ are divided by $2\sqrt{|\alpha|}$ and $2|a|$, respectively to get a curve close to a circle of radius 1. The symmetry with respect to the Y axis gives the intersection of $W^s(Q_+)$ with Σ. The values of the radii of these curves can be computed for equispaced values of the argument by Lagrange interpolation using the closest arguments in the computed curve. The difference between the respective radii provides the splitting.

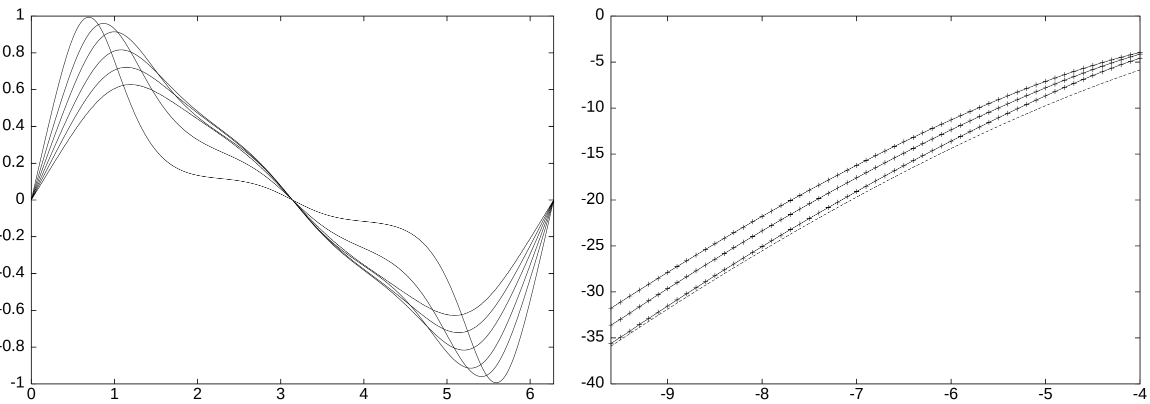

Figure 5: Some details about the two-dimensional splitting. Left: The splitting distance for several values of α as a function of the argument (see the text for explanation about the sample of values for α and the scalings which are considered). Right: The first three harmonics of the two-dimensional splitting (solid lines) and the one-dimensional splitting (dashed line) are displayed (see the text for additional explanation)

Figure 5 shows some results. On the left picture we display a sample for values of α from -4 to -8 with stepsize -1. The splitting is shown as a function of the argument with origin on the Y-axis. In the plot, when $|\alpha|$ increases, the maxima decrease and move to the right. To show all these curves in the same plot the values of the splitting have been multiplied by 25, 825, 6×10^4, 8×10^6, 1.9×10^9 and 7.5×10^{11}.

To summarize the information we have also made the Fourier analysis of the splitting function for a set of values going from -4 to -9.6 with step -0.1. The right part of Figure 5 shows the first three harmonics (due to the odd character they are sinus terms) where the amplitudes are given in logarithmic scale and decrease when the order of the harmonic increases. For comparison purposes we include also, as a discontinuous line, the splitting for the one-dimensional invariant manifolds as shown in Figure 3. We see that the one-dimensional splitting is below the third harmonic of the splitting of the two-dimensional invariant manifolds. Furthermore when the one-dimensional splitting is seen in Σ after $W^u(Q_+)$ passing close to Q_-, it is roughly squared. Hence the one-dimensional splitting is much less than the two-dimensional one. This confirms the numerical evidences which will be presented in Section 4.3 about the existence of Shilnikov homoclinic orbits in a neighbourhood of the HZ^* singularity.

Remark 3.10 We do not include neither explorations (in quadruple precision) of the two-dimensional splitting for larger values of $|\alpha|$ nor the study when $\beta \neq 0$. Essentially the role of β is to move the splitting function upwards when $\beta > 0$ and downwards when $\beta < 0$. It seems that this motion is almost linear in β. It would be possible to obtain a curve in (α, β) where there is a tangency between $W^u(Q_-)$ and $W^s(Q_+)$.

The Michelson system is the only unfolding of the HZ^* singularity where a precise estimation of the splitting of the one dimensional invariant manifolds has been calculated. In [39] the authors consider the equation:

$$\delta w''' + w' = 1 - w^2 \tag{3.9}$$

which is equivalent to the Michelson system (1.7) and prove the following result

Theorem 3.11 [39] *For the unique solution $\omega(t)$ satisfying $\omega(0) = 0$, $\omega'(0) > 0$ on $[0, \infty)$ and $\omega(\infty) = 1$ we have*

$$w''(0) \sim -A\delta^{-2} \exp\left(\frac{-\pi}{2\sqrt{\delta}}\right),$$

as $\delta \to 0^+$ for some positive constant A.

Note that due to the reversibility of the system the above expression gives the one dimensional splitting function. Indeed, taking coordinates $X = \omega$, $Y = \omega'$ and $Z = \omega''$, the above theorem gives the Z coordinate of the intersection point of the (one dimensional) unstable manifold of the equilibrium point at $(X, Y, Z) = (1, 0, 0)$ with the plane $X = 0$. Therefore, due to the reversibility, the Z coordinate of the intersection point of the (one dimensional) stable manifold of the equilibrium point at $(X, Y, Z) = (-1, 0, 0)$ with the plane $X = 0$ is estimated by $A\delta^{-2} \exp\left(\frac{-\pi}{2\sqrt{\delta}}\right)$. Hence the splitting function is given by $2A\delta^{-2} \exp\left(\frac{-\pi}{2\sqrt{\delta}}\right)$.

Taking into account the correspondent rescalings we get that the parameter ε introduced in (2.3) and the parameters α, λ and δ as given in (3.6), (1.6) and (3.9), respectively, are related by

$$|\alpha| = |\lambda|^{-1/3} = \delta^{-1/3} = \varepsilon^{-2/3}.$$

Particularly after applying the blow-up (2.3) and the scaling (2.5) to the normalized Michelson system as given in (2.12) (with $\nu = 0$), the splitting function between the one dimensional invariant manifolds is given by

$$\|S^{(1)}(\varepsilon)\| = C\varepsilon^{-2} \exp(-\frac{\pi}{2\varepsilon}) + o(\exp(-\frac{\pi}{2\varepsilon})),$$

for some positive constant C. Moreover the splitting function in system (3.6) is given by

$$\|S^{(1)}(\alpha)\| = C|\alpha|^4 \exp(-\frac{\pi}{2}|\alpha|^{3/2}) + o(\exp(-\frac{\pi}{2}|\alpha|^{3/2})).$$

for some positive constant C. To get the above expression we also have to use that w in equation (3.9) and Z in system (3.6) are related by $w'' = -\alpha^2 Z$.

Note that the previous numerical results agree with the above estimations.

Remark 3.12 Applying the formulas in [2] to expression (2.12) it follows that

$$\|S^{(1)}(\lambda)\| = C|\lambda|^{-1/2}\exp(-\frac{\pi}{2|\lambda|^{1/2}}) + o(\exp(-\frac{\pi}{2|\lambda|^{1/2}})).$$

for some positive constant C. Taking into account that Z, α in (3.6) and z, λ in (1.6) are related by $Z = -(|\lambda|)^{5/6}z$ and $|\alpha| = |\lambda|^{-1/3}$, respectively, it follows that the above expression for the splitting agrees with (3.7).

3.6 A mild splitting condition and its consequences

In §3.4 we have checked numerically in several examples that the dominant term for the modulus of the splitting function $S^{(1)}(\bar{\mu},\varepsilon)$ is of the type $C\varepsilon^n\exp(-\gamma/\varepsilon)$ where C, n and γ are real constants and moreover C and γ are strictly positive. In fact, applying the results in [2] (see Remark 3.9), we know that $n = -(1+a)$ and $\gamma = \pi/2$. On the other hand we know that the splitting function $S^{(2)}(\varphi,\bar{\mu},\varepsilon)$ for the two dimensional invariant manifolds can be written as the sum of a function $S_{\mathrm{f}}^{(2)}(\bar{\mu},\varepsilon) = \alpha_1\bar{\mu} + \alpha_2\varepsilon + O(\|(\bar{\mu},\varepsilon)\|)$ with $\alpha_1 \neq 0$ and a function $S_{\mathrm{b}}^{(2)}(\varphi,\bar{\mu},\varepsilon)$ which tends to zero when $\varepsilon \to 0$ beyond all orders. In the numerical experiments we have seen that the dominant term in $S_{\mathrm{b}}^{(2)}(\varphi,\bar{\mu},\varepsilon)$ is of the type $C\varepsilon^n\exp(-\gamma/\varepsilon)f(\varphi)$, where again C, n and γ are real constants with C and γ strictly positive and where f is a 2π periodic function. Denote by $C^s(\bar{\mu},\varepsilon)$ and $C^u(\bar{\mu},\varepsilon)$ the closed curves determined by the first intersection of $W^s(\bar{p}_+)$ and $W^u(\bar{p}_-)$, respectively, with $\bar{z} = 0$. Both curves can be parametrized by the variable φ and we assume that $S^{(2)}(\varphi,\bar{\mu},\varepsilon) > 0$ (resp. $S^{(2)}(\varphi,\bar{\mu},\varepsilon) < 0$) when, for that value of φ, $C^u(\bar{\mu},\varepsilon) \in \mathrm{Ext}(\mathrm{C^s}(\bar{\mu},\varepsilon))$ (resp. $C^s(\bar{\mu},\varepsilon) \in \mathrm{Ext}(\mathrm{C^u}(\bar{\mu},\varepsilon))$).

In this section we will show that by only assuming mild conditions on upper and lower bounds for the exponentially small factors, one can prove the accumulation of Shilnikov homoclinic orbits and, in the reversible case, the accumulation of Bykov cycles.

More precisely we will assume that:

(S1) There exist real constants $C_1 > 0$, N_1 and $\gamma_1 > 0$ such that

$$0 < \|S^{(1)}(\bar{\mu},\varepsilon)\| \leq C_1\varepsilon^{N_1}\exp(-\gamma_1/\varepsilon) \tag{3.10}$$

for all $\bar{\mu}$ and $\varepsilon > 0$ small enough.

(S2) Let

$$M(\bar{\mu},\varepsilon) = \max_{\varphi\in[0,2\pi]}\mathrm{S}_{\mathrm{b}}^{(2)}(\varphi,\bar{\mu},\varepsilon).$$

There exist real constants $C_2 > 0$, N_2 and $\gamma_2 > 0$ such that

$$C_2\varepsilon^{N_2}\exp(-\gamma_2/\varepsilon) \leq M(\bar{\mu},\varepsilon) \tag{3.11}$$

as $\varepsilon \to 0$ uniformly in $\bar{\mu}$ and φ.

We are assuming that both the one-dimensional and the two-dimensional invariant manifolds of the equilibrium points split. To study the existence of homoclinic orbits at $\bar{p}_+$ we have to follow the one dimensional invariant manifold by the forward flow and pay attention to the subsequent intersections with the plane $z = 0$.

Let $q_0(\bar\mu,\varepsilon)$ be the first intersection point of $W^u(\bar p_+)$ with the plane $\bar z = 0$. The hypotheses (S1) implies that the one-dimensional invariant manifolds split. Hence we can define the first intersection point $\bar q_0(\bar\mu,\varepsilon)$ of the forward orbit of $q_0(\bar\mu,\varepsilon)$ with $\bar z = 0$. Let $\varphi_{\bar q_0}(\bar\mu,\varepsilon)$ be the C^∞ function providing the argument when $\bar q_0(\bar\mu,\varepsilon)$ is written in polar coordinates.

Theorem 3.13 *Consider a one-parameter unfolding of the HZ* singularity as in (3.1) with $\bar\mu = \bar\mu(\varepsilon)$ given as a C^∞ function of ε such that $\bar\mu(0) = 0$. Assume that hypotheses (S1) and (S2) are satisfied and moreover that:*

(S3) $\left|S_{\mathrm{f}}^{(2)}(\bar\mu(\varepsilon),\varepsilon)\right| < \widetilde{C}_2\varepsilon^{N_2}\exp(-\gamma_2/\varepsilon)$ *where $\widetilde{C}_2 < C_2$ is a positive constant and C_2, N_2 and γ_2 are those given in (S2).*

(S4) $\gamma_2/\gamma_1 < 2/a$.

(S5) There exists a C^∞ function $\varphi_0(\varepsilon)$ such that $S_{\mathrm{b}}^{(2)}(\varphi_0(\varepsilon),\bar\mu(\varepsilon),\varepsilon) = 0$ for ε small enough and $|\varphi_{\bar q_0}(\bar\mu(\varepsilon),\varepsilon) - \varphi_0(\varepsilon)|$ tends to infinity as $\varepsilon \to 0$.

Then, for $0 < a < 2$, there exists a sequence of parameter values $\{\varepsilon_n\}$ with $\varepsilon_n \to 0$ as $n \to \infty$ such that the corresponding system at $(\bar\mu(\varepsilon_n),\varepsilon_n)$ has a Shilnikov homoclinic orbit at $\bar p_+$ which intersects $\bar z = 0$ only at two points.

Remark 3.14 The assumption (S5) means that the point $\bar q_0$ turns around the $\bar z$ axis, close to the intersection of $W^s(\bar p_+)$ with $\bar z = 0$, faster then the heteroclinic point $\varphi_0(\varepsilon)$. This will be essential to prove the existence of infinitely many values of ε, when $\varepsilon \to 0$, for which $W^u(\bar p_+) \subset W^s(\bar p_+)$.

Proof. As mentioned in §3.1, either when $\bar z \geq 0$ or when $\bar z \leq 0$ one can introduce cylindrical coordinates in (3.1). Using that $\bar\mu(\varepsilon) = O(\varepsilon)$, such family can be written as an $O(\varepsilon)$ perturbation of an integrable system with integrating factor $r^{\left(\frac{2}{a}-1\right)}$ and first integral

$$H(r,z) = r^{2/a}\left[1 - z^2 - \frac{b}{a+1}r^2\right].$$

Taking into account that $0 < a < 2$ one can easily prove that $dH/dt = O(\varepsilon)O(\bar r^{2/a})$. On the other hand, for any fixed positive value h close enough to 0, the equation $H(\bar r, 0) = h$ has two solutions, $\bar r_1(h) = h^{a/2} + o(h^{a/2})$ and $\bar r_2(h) = \bar R - Kh + o(h)$, with $\bar R = \sqrt{\frac{a+1}{b}}$ and $K = \frac{1}{2}\frac{1+a}{b}\bar R^{a/(2+a)}$. It follows that $\bar R - \bar r_2 = K\bar r_1^{2/a} + o(\bar r_1^{2/a})$. Consequently, for any $\delta > 0$ and $q \in \{\bar z = 0\}$, if $\|q\|$ and ε are small enough, then

$$\bar R - \|\bar q\| < (K+\delta)\|q\|^{\frac{2}{a}}, \tag{3.12}$$

where $\bar q$ denotes the first intersection point of the orbit of q with the plane $\bar z = 0$ for strictly positive time. Note that for $h = H(q,0)$ and $\bar h = H(\bar q, 0)$, $\bar h = h + O(\varepsilon)O(h)$. The above expression gives an upper bound for the distance between $\bar q$ and the curve given by the first intersection between $W^u(\bar p_-)$ and $\{\bar z = 0\}$, since we can take an ε-dependent change of coordinates, being the identity for $r = 0$, to fix $W^u(\bar p_-)$ on the ellipsoid $\left(r/\bar R\right)^2 + \bar z^2 = 1$.

From (3.12) and hypothesis (S1) it follows that, if ε is small enough the distance between $\bar{q}_0(\bar{\mu}(\varepsilon),\varepsilon)$ and $C^u(\bar{\mu}(\varepsilon),\varepsilon)$ will be bounded from above by a function

$$\overline{C}_1\varepsilon^{\overline{N}_1}\exp(-2\gamma_1/a\varepsilon), \tag{3.13}$$

with real constants $\overline{C}_1 > 0$ and $\overline{N}_1$.

On the other hand

$$\begin{aligned} \max_{\varphi\in[0,2\pi]}S^{(2)}(\varphi,\bar{\mu}(\varepsilon),\varepsilon) &= \max_{\varphi\in[0,2\pi]}(S_{\mathrm{f}}^{(2)}(\bar{\mu}(\varepsilon),\varepsilon)+S_{\mathrm{b}}^{(2)}(\varphi,\bar{\mu}(\varepsilon),\varepsilon)) \\ &\geq \max_{\varphi\in[0,2\pi]}\left(S_{\mathrm{b}}^{(2)}(\varphi,\bar{\mu}(\varepsilon),\varepsilon)-\left|S_{\mathrm{f}}^{(2)}(\bar{\mu}(\varepsilon),\varepsilon)\right|\right) \\ &= \max_{\varphi\in[0,2\pi]}\left(S_{\mathrm{b}}^{(2)}(\varphi,\bar{\mu}(\varepsilon),\varepsilon)\right)-\left|S_{\mathrm{f}}^{(2)}(\bar{\mu}(\varepsilon),\varepsilon)\right| \\ &\geq (C_2-\widetilde{C}_2)\varepsilon^{N_2}\exp(-\gamma_2/\varepsilon), \end{aligned}$$

where we have used hypotheses (S2) and (S3) to get the last inequality.

From (S4) we conclude that the distance between $\bar{q}_0(\bar{\mu}(\varepsilon),\varepsilon)$ and $C^u(\bar{\mu}(\varepsilon),\varepsilon)$ is always below the maximum distance between $C^u(\bar{\mu}(\varepsilon),\varepsilon)$ and $C^s(\bar{\mu}(\varepsilon),\varepsilon)$ computed for values of φ such that $C^u(\bar{\mu},\varepsilon)\in \mathrm{Ext}(C^s(\bar{\mu},\varepsilon))$. Hypothesis (S5) implies that $\bar{q}_0(\bar{\mu}(\varepsilon),\varepsilon)$ must intersect $C^s(\bar{\mu}(\varepsilon),\varepsilon)$ infinitely many times as $\varepsilon\to 0$ and hence the result follows. □

Remark 3.15 Typically we expect that $\gamma_1=\pi/2$ in (3.10) and $\gamma_2=\pi/(2a)$ in (3.11). Note that, in such case, (S4) is fulfilled.

Remark 3.16 In the reversible case, assumption (S5) is straightforward.

Corollary 3.17 *The conclusion of Theorem 3.13 holds for any one-parameter conservative unfolding with $0<a<2$ under conditions (S1), (S2), (S4) and (S5).*

Proof. In the conservative case $\bar{\mu}(\varepsilon)\equiv 0$ and the hypothesis (S3) is always satisfied. Otherwise one of the curves determined by the first intersection of the two-dimensional invariant manifolds with $\bar{z}=0$ should enclose the other. □

Corollary 3.18 *Consider a two-parameter $(\bar{\mu},\varepsilon)$-unfolding of the HZ* singularity as given in (3.1) and assume that $\alpha_1=(\partial S_{\mathrm{f}}^{(2)}/\partial\bar{\mu})(0,0)\neq 0$. For ε small enough, let $\xi(\varepsilon)$ be a C^∞ function with $\xi(0)=0$ satisfying $S_{\mathrm{f}}^{(2)}(\xi(\varepsilon),\varepsilon)=0$ and define*

$$\Omega=\left\{(\bar{\mu},\varepsilon)\ \mid\ |\bar{\mu}-\xi(\varepsilon)|<K\varepsilon^{N_2}\exp\left(-\gamma_2/\varepsilon\right)\right\},$$

where $K<C_2/|\alpha_1|$. If $0<a<2$ and (S1), (S2), (S4) and (S5) are satisfied then the conclusion of Theorem 3.13 follows for any one-parameter unfolding given by a C^∞ curve in Ω parameterized with respect to ε and emanating from $(\bar{\mu},\varepsilon)=(0,0)$.

Proof. Let $\bar{\mu}(\varepsilon)$ be a C^∞ function $\bar{\mu}(\varepsilon)$ with $\bar{\mu}(0)=0$ and $(\bar{\mu}(\varepsilon),\varepsilon)\in\Omega$ for ε small enough. Clearly, for some δ as small as required if ε is small enough,

$$\begin{aligned} \left|S_{\mathrm{f}}^{(2)}(\bar{\mu}(\varepsilon),\varepsilon)\right| &= \left|S_{\mathrm{f}}^{(2)}(\bar{\mu}(\varepsilon),\varepsilon)-S_{\mathrm{f}}^{(2)}(\xi(\varepsilon),\varepsilon)\right| \\ &\leq (|\alpha_1|+\delta)\,|\bar{\mu}(\varepsilon)-\xi(\varepsilon)| \\ &\leq (|\alpha_1|+\delta)K\varepsilon^{N_2}\exp\left(-\gamma_2/\varepsilon\right). \end{aligned}$$

Let $\widetilde{C}_2 = (|\alpha_1| + \delta)K$. Since for δ small enough $K < (C_2/(|\alpha_1| + \delta))$ it follows that $\widetilde{C}_2 < C_2$. Hence the hypothesis (S3) in Theorem 3.13 is also satisfied and the result follows. □

Remark 3.19 Note that if one of the above results is applicable then, following the classical results in [21], there will appear subsidiary sequences of Shilnikov homoclinic orbits with more than two intersections with the plane $z = 0$.

Remark 3.20 Consider a family in the class of reversible unfoldings introduced in §3.3. Assuming that conditions (S1) and (S2) are satisfied, the same arguments used in the proof of Theorem 3.7 permit us to prove the accumulation of Bykov cycles at the HZ^* bifurcation point. Note that we have to understand such cycles in a weaker sense since (S2) says nothing about transversality of the two dimensional invariant manifolds.

4 Michelson system

4.1 Summary of known results

As already mentioned in §1.4, there is a long list of papers devoted to the study of the Michelson system (1.7). We will only pay attention to the most relevant results which are valid in a range of parameters close to $c = 0$. Recall (see §2.4) that when $c = 0$ the system possesses a HZ^* singularity. More general background discussions can be found in [33, 34, 37, 49]. Let us recall that (1.7) is equivalent to the extended Michelson system (1.6) with $\nu = 0$. Note also that, as explained in §2.4, we can introduce new coordinates to write (1.6) in the form (2.12) and also work with equivalent families like (3.1) or (3.2) for which the splitting functions $S^{(1)}(\bar{\mu}, \varepsilon)$ and $S^{(2)}(\varphi, \bar{\mu}, \varepsilon)$ were introduced in §3.4. When working with such expressions, the Michelson system corresponds to $\bar{\mu} = 0$, and the splitting functions only depend on the parameter ε.

In [27] it is proved that for all $c > 0$ there is no solution of (1.7) with $x(t)$ monotone and connecting the equilibrium points along the one dimensional invariant manifolds. It follows from such result that

(M1) $S^{(1)}(\varepsilon) \neq 0$ for all $\varepsilon > 0$.

An explicit estimation of the splitting function for the one-dimensional invariant manifolds is provided in [39]. As already explained in §3.4 we get

(M2) $\|S^{(1)}(\varepsilon)\| = C\varepsilon^{-4}\exp(-\pi/2\varepsilon) + o(\exp(-\pi/2\varepsilon))$.

On the other hand all heteroclinic connections between the equilibrium points along the two-dimensional invariant manifolds (only hitting $z = 0$ once) must be invariant under the involution (see [1] and [51]). This implies that if they hit the plane $z = 0$ only once then they must cross the reversibility axis $x = z = 0$. Since the two-dimensional invariant manifolds cut the plane $z = 0$ on closed curves which tend to a circle which is invariant by the reversibility, it follows that, as already argued in [33], for ε small enough they must coincide in exactly two points, where the intersections are at least topologically transversal. Note that otherwise one of the curves should be enclosed by the other which is not possible due to the reversibility. The contact is, because of the analyticity, either transversal or of some odd degree. It follows that

(M3) $S^{(2)}(\varphi, \varepsilon))$ has exactly two zeros for ε small.

Nevertheless, as far as we know, in the literature there is no estimation of the maximum variation of the $|S^{(2)}(\varphi, \varepsilon)|$.

The accumulation of Bykov cycles to the Hopf-zero singularity was proved in [33]. As explained above there are exactly two heteroclinic connections (only hitting $z = 0$ once) along the two-dimensional invariant manifolds. Authors in [33] show that in the case of an odd order degree there must exist transversal intersections nearby. The existence of heteroclinic connections along the one-dimensional invariant manifolds follows from (M1) and the fact that the two-dimensional invariant manifolds do split (M3). Hence one can apply Theorem 3.7 to conclude the accumulation of Bykov cycles.

Remark 4.1 We have used Theorem 3.7 to show the existence of Bykov cycles. The argument used in [33] is based on [1], where the existence of many heteroclinic connections (intersecting the plane $z = 0$ twice) is argued. Nevertheless a similar idea to that used in the proof of Theorem 3.7 is also mentioned in [33]. However one should notice that the arguments used in the proof of that theorem also show that the speed of rotation of the second intersection point of $W^u(\bar{p}_+)$ with $z = 0$ is nowhere zero. Hence the intersections with the fixed point set of the involution occur with positive speed. This is a detail which the authors in [33] leave unverified, although the conclusions, as they explain, remain valid.

Remark 4.2 In [1] the authors also discussed the existence of homoclinic connections with only two intersections with the plane $z = 0$.

Remark 4.3 Analysis of periodic orbits in (1.7) can be found for instance in [37] (where also the existence of invariant tori is discussed numerically) and [30]. Nevertheless no complete analysis, as that we will present in §4.3, is provided for parameter values close to $c = 0$.

4.2 Application of theoretical results

As already mentioned in §4.1, Theorem 3.7 can be applied to prove the accumulation of Bykov cycles in the Michelson system but this result was already proved in [33].

Consider the extended Michelson system (1.6) and let us discuss the applicability of Theorem 3.3. In the sequel we will assume that system (1.6) is written in the form (2.7). We already know that the condition on the coefficient a is satisfied in the case of the Michelson system (see §2.4). From (M1) we know that the exceptional set is empty when $\bar{\mu} = 0$ but of course this is not enough to apply the result. Nevertheless the numerical results in §3.4 about the splitting function for the one-dimensional invariant manifolds show that the exceptional set reduces to the line $\varepsilon = 0$ in a neighbourhood of $(\bar{\mu}, \varepsilon) = (0, 0)$. Therefore, for $\bar{\mu}_0$ as indicated in Theorem 3.3 and ε small enough, we can conclude that in each path connecting parameter points in forward and backward trapping there exist parameter values for which the system has a primary Shilnikov homoclinic orbit (with only two intersections with $\bar{z} = 0$).

On the other hand if we take into account (M2) and again the numerical results provided in §3.4 about the splitting function for the two-dimensional invariant manifolds it follows that hypotheses (S1), (S2) and (S4) in Corollaries 3.17 and 3.18 are satisfied. From the former we know that there exists a sequence of parameter values for which the Michelson system has a primary Shilnikov homoclinic orbit and that the sequence tend to 0. Applying Corollary 3.18 to the extended Michelson system we know that there exists an exponentially small wedge around the reversibility axis such that the same conclusion follows along any curve in the wedge emanating from $(\bar{\mu}, \varepsilon) = (0, 0)$.

Remark 4.4 Under generic assumptions, any parameter value for which a system has a Bykov cycle is an accumulation point of parameter values corresponding to Shilnikov homoclinic orbits. Hence the accumulation of Bykov cycles at the Hopf-zero point in the Michelson system, as proved in [33], implies the accumulation of Shilnikov homoclinic orbits. Nevertheless, in contrast with their result, one should notice that our arguments provide primary Shilnikov homoclinic orbits. The heteroclinic connections along the one-dimensional invariant manifolds which are part of the Bykov cycles in [33] have three intersection with $z = 0$. Hence the associated Shilnikov homoclinic orbits has four intersections and therefore they are of secondary type.

Remark 4.5 Note that primary Shilnikov homoclinic orbits occur in the Michelson system at isolated parameter values. Hence we can choose paths to apply Theorem 3.3 avoiding the parameter values for which the Michelson system has a primary Shilnikov homoclinic orbit. Therefore our result of existence provides parameter values for which the system has non-zero divergence.

4.3 Dynamics: numerical results

Along this section we will consider the system (3.6) which is equivalent to the extended Michelson system (1.6) when $\lambda < 0$ and $\nu \in \mathbb{R}$ and present an extensive numerical study which help to understand the dynamics arising from the Hopf-Zero singularity.

4.3.1 Dynamics in the conservative case

First we consider $\beta = 0$ in (3.6). For convenience, dynamical behaviour will be described with respect to the parameter $\lambda = \alpha^{-3}$ as shown in system (1.6). It follows from [36] that when $\lambda \to -\infty$ the maximal compact invariant set of (3.6) reduces to the set consisting of the two equilibrium points and a unique intersection between their two dimensional invariant manifolds. According to [34] there is saddle-node bifurcation at $\lambda \approx -0.80163$ where two periodic orbits appear, one of them is of saddle type and the other elliptic. This is the first parameter value for which non-escaping regions emerge. As $\lambda \to 0$ the size of this regions increases as long as the family approaches the Hopf-zero bifurcation point.

In order to study the abundance of non-escaping orbits we take a Poincaré section on $Z = 0$ with $\dot{Z} > 0$. Scaling Y by the factor $2\sqrt{|\lambda|^{1/3}}$ we reduce to a domain which is approximately the half unit disk (it approaches the half unit disk as $|\lambda| \to 0$). Initial points are taken on the domain $(Y, X) \in [-1, 0] \times [-1.05, 1.05]$. Transversality is lost along a curve which does not play any role. Note that the Poincaré map preserves a measure whose density is proportional to $\dot{Z}$ on $Z = 0$ and, hence it is absolutely continuous with respect to the Lebesgue measure on the (y, x) plane.

Starting on the given domain the points in a fine equispaced grid which do not escape are stored. As a simple measure we have taken this number of points. When $|\lambda| \to 0$ the measure of the set of subsisting points has a finite limit (see Figure 6 left). To better see the details values have been multiplied by $|\lambda|$ (see Figure 6 right). The marks from 2 to 10 at the bottom part of the plot denote the bifurcations of islands with rotation number $1:2, \ldots, 1:10$. The marks form 5 to 10 along the curve denote the places at which invariant curves confining the islands are broken.

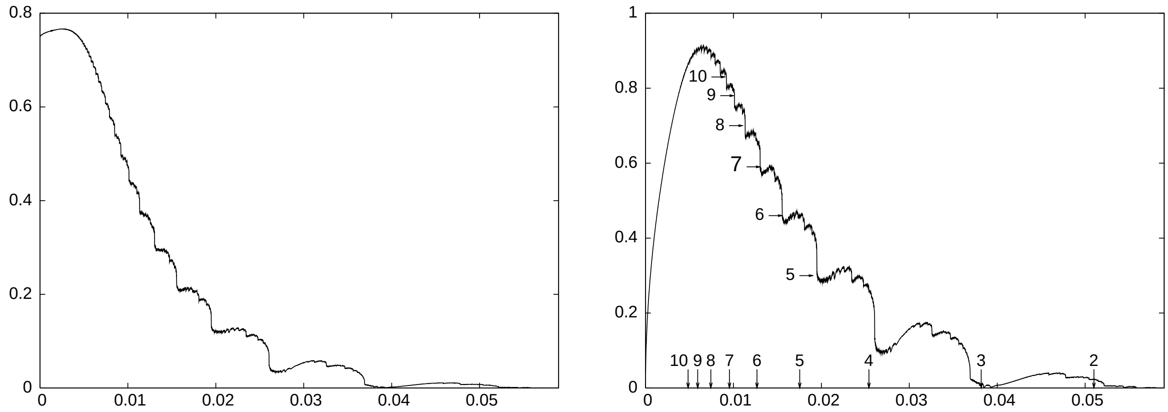

Figure 6: Left: Statistics of the number of points which do not scape as a function of $|\lambda|$ using a 4000×4200 grid. Right: The values have been multiplied by $|\lambda|$, to better see the details. The location of some resonances both, at the central elliptic fixed point and at the breakdown of invariant curves which disconnects the related islands is shown.

On Figure 7 we show the changes in the set of non escaping points which occur for some small changes in $|\lambda|$. Namely, we have included three transitions corresponding to the jumps associated to periods 3 (top left), 4 (top right) and 5 (bottom) in Figure 6 (right). On Figure 7 (top left) we see that when $|\lambda| = 0.03692$ there appears a stable region, bounded by an invariant curve which encloses the islands of period 3, and many chains of islands outside the curve. These are the points in gray in the plot. Note that the points in black are hiding points in gray. Beyond period-3 elliptic points inside the islands, one can guess the existence of a period-3 hyperbolic orbit. The transversal homoclinic intersection of its manifolds creates a chaotic zone, but the points on it can not escape because of the invariant curve surrounding the whole structure. Changing to $|\lambda| = 0.03693$ the curves surrounding the chaotic zone break down. Hence points in the chaotic zone can (and they do) escape. The non escaping points for this value of λ are plotted in black. One can see a central area around the the fixed elliptic point, with very sharp boundaries and the big period-3 islands. These are surrounded by chains of tiny islands. Also chains of islands can be seen surrounding the set of period-3 islands. The major islands of theses chains have only minor changes with respect to the islands found for $|\lambda| = 0.03692$. Transitions corresponding to jumps associated to periods 4 and 5 should be understood similarly. A movie showing a collection of transitions along a sequence of parameters is available in `http://www.maia.ub.es/dsg/moviehsn`. A discussion of the mechanism explaining the escape of points and their relation with the break down of invariant curves is included in [43] in the context of area preserving maps. See also [42] for a variety of problems with similar properties in different contexts.

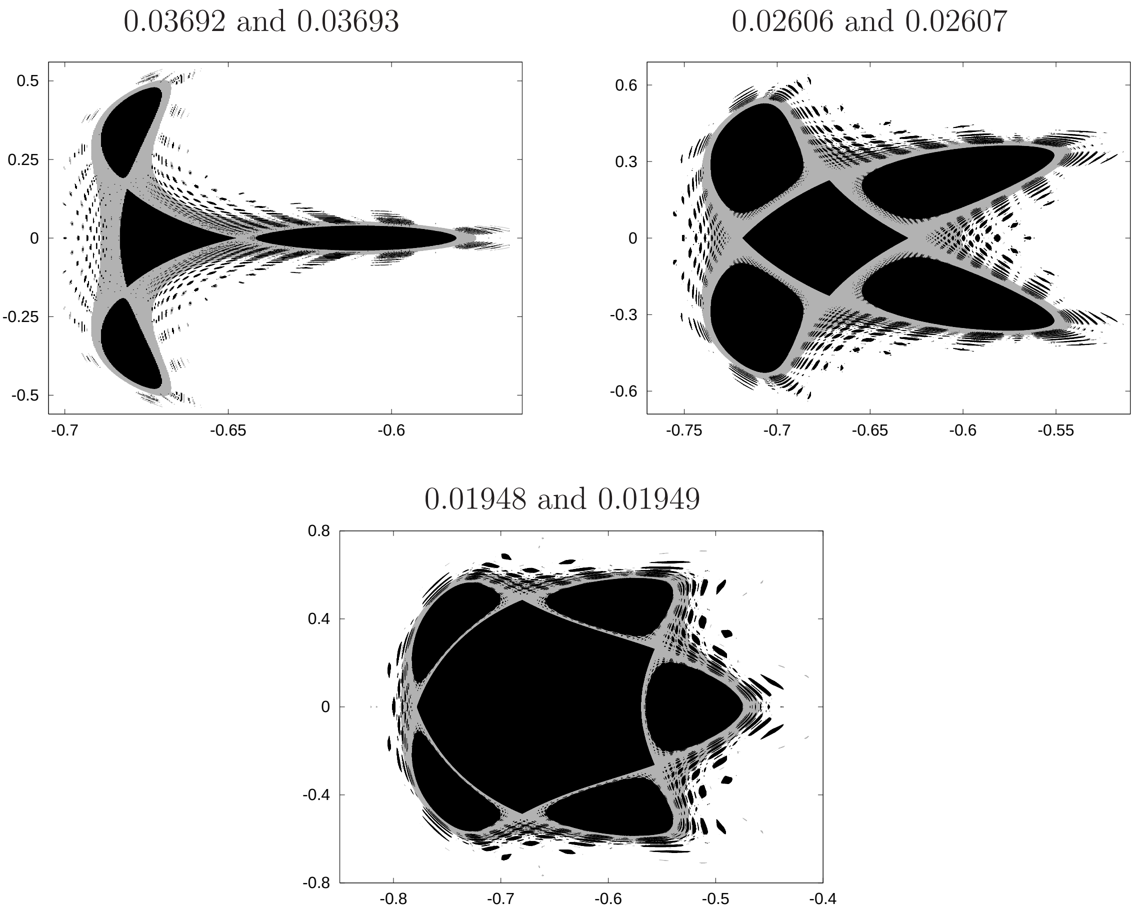

Figure 7: Transitions corresponding to jumps associated to periods 3 (top left), 4 (top right) and 5 (bottom) in Figure 6 (right). In each case non escaping points for the smallest (resp. largest) value of $|\lambda|$ are plotted in gray (resp. black). Note that points in black are hiding points in gray.

4.3.2 Dynamics in the dissipative case with constant divergence

To illustrate the effect of adding a small dissipation, Figure 8 displays (in gray) invariant curves and islands for the conservative case with $|\lambda| = 0.011$ ($\alpha \approx -4.496$) and also attracting periodic orbits (points in black) when dissipation is set to $\beta = -10^{-4}$. Again we are taking a transverse section on $Z = 0$ with $\dot{Z} > 0$ and the plotted variables are $(Y/e, X)$, with $e = 2\sqrt{|\lambda|}$. Most of the initial conditions are taken on $X = 0$. Other points escape after transients that can be as long as 12×10^4 iterates. See [44] for the mechanisms leading to the appearance of islands outside the main confined region.

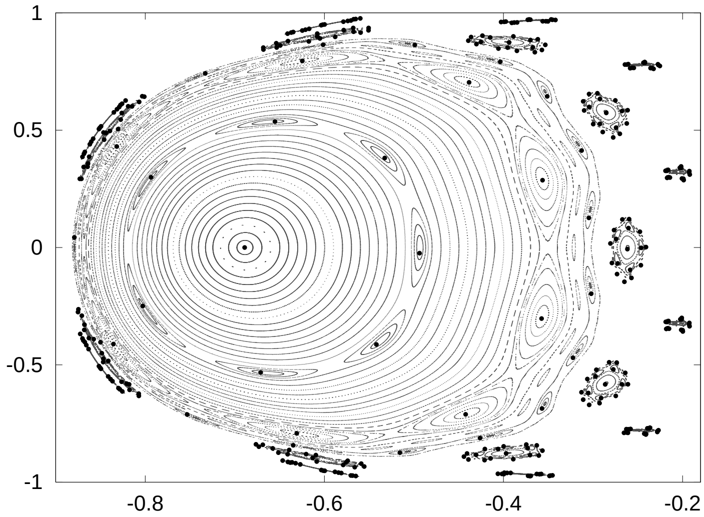

Figure 8: Invariant curves and islands (in gray) for the conservative case with $|\lambda| = 0.011$. Points in black correspond to attracting periodic orbits with different rotation numbers with divergence $\beta = -10^{-4}$.

The initial points are taken on the $X = 0$ axis, using values of the form $Y = je \times 10^{-4}$ with $j = 1, \ldots, 10^4$. Beyond the fixed point, attracting periodic orbits with periods $7, 8, 17, 9, 45, 99, 150$ and rotation numbers $\rho = 1/7, 1/8, 2/17, 1/9, 1/9, 1/9, 1/10$, respectively, are found. Note that some of them can be seen as obtained, by evolution from the conservative case, of elliptic periodic orbits in satellite islands. The respective abundances of initial points captured by the fixed point and the different periodic orbits are, respectively, $6157, 325, 134, 14, 319, 112, 5, 1$, The other 2933 points escape. The results can change with tiny changes in the initial conditions, because the basins of attraction of the different attractors are extremely wrapped.

It is also remarkable that some of the attracting periodic orbits are not close to any island of the conservative case. This is easy to explain. The elliptic point at the center of an island can become hyperbolic, leading to the usual period doubling cascade of conservative systems and destroy the island. However a tiny dissipation, specially in the case of large period, is able to convert an unstable saddle into a stable focus.

Existence of Shilnikov homoclinic orbits in unfoldings of the HZ^* singularities is one of the main motivations for our paper. To get information about values of the parameters for which they occur in the extended Michelson system (3.6) we study for which values of (α, β) the one-dimensional invariant manifold $W^u(Q_+)$ intersects the section $\Sigma = \{(X, Y, Z) \in \mathbb{R}^3 \,|\, g(X, Y, Z) = 0\}$ with g as defined in (3.8). Figure 9 displays this information. The white zones correspond to escape after two intersections. We also see that the maximum admissible values of β without escaping are of the order of the magnitude of the splitting of the one-dimensional invariant manifolds.

A more detailed information is given in Figure 10. The gray region on the left corresponds to parameter values with $W^u(Q_-)$ having at least three intersections with Σ. Note that now β is in its real scale and the range of $|\alpha|$ is small. The boundary curve in black corresponds to "primary" Shilnikov homoclinic orbits associated to Q_+. The number of oscillations of the boundary of the gray region is increasing quickly when $\alpha \to -\infty$. Let $\beta = q(\alpha)$ be the function defining this boundary. The right part of Figure 10 displays α in the horizontal axis and the number of zeros of q between -4 and an arbitrary value of $\alpha \in [-8.5, -4]$. A fit of the number of zeros of q between -4 and α is of the form $n = c_1|\alpha|^{c_2} - c_3$ with c_1, c_2 and c_3 positive constants and $c_2 \approx 3$.

To be able to find "visible" domains with strange attractors, one has to take relatively large values of $|b|$. The reason is clear. The fixed point of the conservative system becomes unstable for $\lambda = \lambda_c \approx -0.051002$, when it has a period doubling. The end of the period doubling cascade is found for $|\lambda| \approx 0.0589$. For $|\lambda| = |\lambda_c|$ and slightly larger values invariant curves still exist around the fixed point. They seem to persist until $|\lambda| \approx 0.05105$. From that point on, most points in a neighbourhood of the fixed point escape. This is due to the fact that the unstable manifold of the fixed point intersects transversally the stable manifold of Q_+.

However, a small dissipation is able to convert the elliptic fixed point into a stable focus. Later on it, when increasing $|\lambda|$, it becomes a saddle. Its unstable manifold is close to the one in the conservative case and will also intersect $W^s(Q_+)$ for values close to the ones for which the intersection is found in the conservative case.

To avoid too small ranges in $|\lambda|$ where we can find a period doubling cascade in the dissipative case, ending in strange attractors, we take a strong dissipation. Values like $\beta = -0.1, -0.2, -0.3, -0.4$ have been checked.

Figure 11 (left) shows the first two Lyapunov exponents for $\beta = -0.4$. They have been computed using methods described in [38, 35, 41] and also references therein. Note that

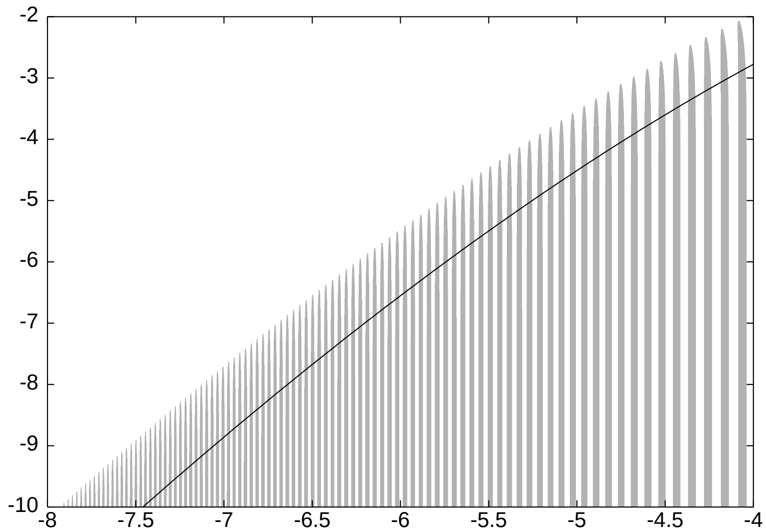

Figure 9: The gray zones show the parameter values for which $W^u(Q_+)$ has at least three intersections with the section Σ. For reference the continuous line gives the size of the half-splitting of the one-dimensional invariant manifolds as given in (3.7). Variables α and $\log_{10}(b)$ are plotted in the horizontal and the vertical axis, respectively

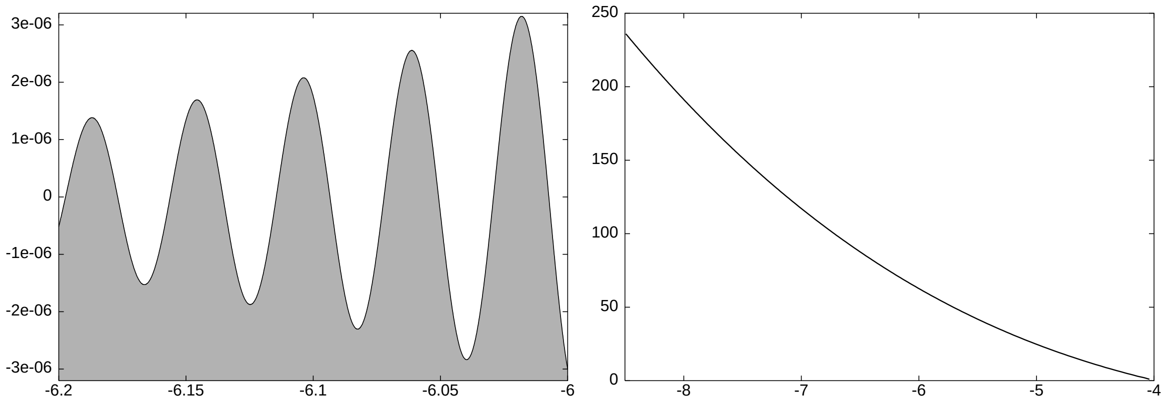

Figure 10: Some details on the escape of $W^u(Q_+)$. Left: The white area corresponds to values of (α, β) for which it escapes after exactly two crossings of Σ. Right: A plot of the number of zeros of the boundary curve on the left part, counted from $\alpha = -4$ downwards.

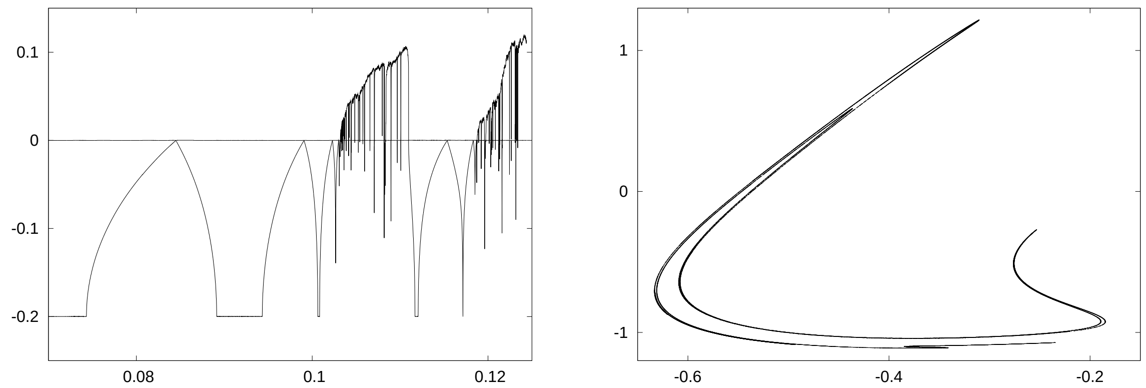

Figure 11: Left: The first two Lyapunov exponents for $\beta = -0.4$. Right: Strange attractor for $|\lambda| = 0.122$.

the value 0 is due to the behaviour along the tangent vector to the orbit. The fixed point in the conservative case became a stable focus, obviously with Lyapunov exponent $\beta/2$. It becomes a stable node around $|\lambda| = 0.07432$ and then a first period doubling occurs near $|\lambda| = 0.08449$. The period doubling cascade is apparent and it ends near $|\lambda| = 0.1032$, where strange attractors start to show up. They are of Hénon-like type. Hence the existence of strange attractors is interrupted by “windows” of attracting periodic orbits.

To compute Lyapunov exponents for a range of values of $|\lambda|$ one can adopt several strategies. For instance, one can start every computation at some give initial point. Typically we take $(X, Y, Z)_0 = (0. - 0.7 \times e, 0)$, where e is the scaling factor introduced above. Another possibility is to take as initial condition the last point computed in the attractor for the previous value of λ. As we have multiple attractors, the results can be different. It is also possible to take several initial conditions for fixed values of the parameters. To produce Figure 11 (left) we have used the first approach. One can observe a sudden jump of the maximal Lyapunov exponent when $|\lambda| = 0.11096$. This is not due to the "destruction" of the previous strange attractor, but to a change in the position of the boundaries of the basin of attraction. One easily checks that in the approximate range $|\lambda| \in [\varepsilon_1, \varepsilon_2] = [0.1109620, 0.1109666]$ the strange attractor coexists with a period 4 attracting periodic orbit. Near $|\lambda| = \varepsilon_1$ a periodic orbit is born by saddle-node bifurcation. Near $|\lambda| = \varepsilon_2$ the stable manifold of the saddle created at $|\lambda| = \varepsilon_1$ destroys the strange attractor. See [40] for the mechanisms of creation/destruction of strange attractors.

Figure 11 (right) shows the current strange attractor for $|\lambda| = 0.122$. Later on, near $|\lambda| = 0.12439$ again $W^s(Q^+))$ is able to destroy definitely the strange attractor.

All the integrations are done using a Taylor method of order 40 with local tolerance 10^{-20}. It allows to obtain 90000 Poincaré iterates per second, in the conservative case, on a 3.2GHz computer.

5 Concluding Remarks

Several questions regarding HZ^* singularities have been considered in this paper. The main technical trouble involved in the study of their unfoldings was made clear from the very beginning introducing normal forms and blow-ups. The fact is that, after scaling, the limiting system is either non regular (2.7) or very degenerate (2.6). As a consequence one even has to wonder whether the invariant manifolds of the equilibrium points can be extended up to the plane $\bar{z} = 0$. It has been shown that a positive answer follows from the results in [3, 4] and therefore it makes sense to consider splitting functions for both the one-dimensional and the two-dimensional invariant manifolds.

Knowing that there exist splitting functions we have obtained theoretical results regarding existence of Shilnikov homoclinic orbits and Bykov cycles. To be precise we have supplied sufficient conditions for their existence using two different approaches. First, introducing the notions of trapping region and exceptional set, a sufficient condition suitable for numerical verification was provided. Second, an existence result was obtained after assuming mild hypotheses for the splitting functions. Roughly speaking such assumptions are related with their exponentially small character. Literature (see [2]) provides a formula to compute the dominant term of the splitting function and it follows that it is indeed exponentially small. Nevertheles the study of the two dimensional splitting function remains open. We have provided numerical evidence of the exponentially small character choosing different perturbation terms in general unfoldings and also focusing on the case of the Michelson system.

Application of theoretical results to the case of the Michelson system has been discussed. Moreover a thorough numerical exploration has also been done for this system. Particularly we have illustrated the evolution of the dynamics in the conservative case and the effect of adding a small dissipation (extended case). Existence of Shilnikov homoclinic orbits and occurrence of chaotic dynamics is also shown for the extended model.

HZ^* singularities are commonly referred to as the most simple singularities (simple in the sense of lowest codimension) unfolding chaotic dynamics. Nevertheless, in this paper we have made clear that an argument valid for any generic unfolding is not yet available. We have provided a sufficient condition which is suitable for numerical validation and an analytical condition which depends on a rigorous control of the splitting functions. Such control is only available in the case of the one dimensional splitting. A thorough analytical study of the two-dimensional splitting remains as a pending task for the future. Note however that according to our results this is the only remaining gap in order to finish the study of the HZ^* singularities.

Acknowledgements

S.I. has been partially supported by the projects MTM2008-06065 and MTM2011-22956. H.K. acknowledges the support of Ministry of Education, Science, Technology, Culture and Sports, Japan, Grant-in-Aid for Scientific Research No. 21340035. C.S. has been partially supported by grants MTM2006-05849/Consolider and MTM2010-16425 (Spain) and 2009 SGR-67 (Catalonia).

References

[1] K. L. Adams, J. R. King and R. H. Tew, Beyond-all-orders effects in multiple-scales asymptotics: travelling-wave solutions to the Kuramoto-Sivashinsky equation, *J. Engineering Math.* **45** (2003), 197–226.

[2] I. Baldomá, O. Castejón and T. M. Seara, Exponentially small heteroclinic breakdown in the generic Hopf-Zero singularity, Preprint.

[3] P. Bonckaert and E. Fontich, Invariant manifolds of maps close to a product of rotations: close to the rotation axis, *J. Differential Equations* **191** (2003), 490–517.

[4] P. Bonckaert and E. Fontich, Invariant manifolds of dynamical systems close to a rotation: transverse to the rotation axis, *J. Differential Equations* **214** (2005), 128–155.

[5] H. W. Broer and G. Vegter, Subordinate Sil'nikov bifurcations near some singularities of vector fields having low codimension, *Ergod. Th. & Dynam. Sys.* **4** (1984), 509–525.

[6] H. W. Broer, C. Simó and R. Vitolo, Bifurcations and strange attractors in the Lorenz-84 climate model with seasonal forcing, *Nonlinearity* **15** (2002) 1205–1268.

[7] H. W. Broer, C. Simó, R. Vitolo, Quasi-periodic Hénon-like attractors in the Lorenz-84 climate model with seasonal forcing, in *Proceedings Equadiff03*, ed. F. Dumortier et al., 601–606, World Scientific, 2005.

[8] H. W. Broer, C. Simó and R. Vitolo, Hopf saddle-node bifurcation for fixed points of 3D-diffeomorphisms: analysis of a resonance bubble, *Physica D* **237** (2008), 1773–1999.

[9] H. W. Broer, C. Simó and R. Vitolo, The Hopf-saddle-node bifurcation for fixed points of 3D-diffeomorphisms: the Arnol'd resonance web, *Bull. Belgian Math. Soc. Simon Stevin* **15** (2008) 769–787.

[10] H. W. Broer, C. Simó, R. Vitolo, Chaos and quasi-periodicity in diffeomorphisms of the solid torus, *Discrete Contin. Dyn. Syst. Ser. B* **14** (2010), 871–905.

[11] H. W. Broer, C. Simó, R. Vitolo, Routes to chaos in the Hopf-saddle-node bifurcation for fixed points of 3D-diffeomorphisms, *Nonlinearity* **23** (2010), 1919–1947.

[12] A. R. Champneys and V. Kirk, The entwined wiggling of homoclinic curves emerging from saddle-node/Hopf instabilities, *Physica D* **195** (2004), 77–105.

[13] F. Dumortier and S. Ibáñez, Nilpotent singularities in generic 4-parameter families of 3-dimensional vector fields, *J. Differential Equations* **127** (1996), 590–647.

[14] F. Dumortier and S. Ibáñez, Singularities of vector fields on $\mathbb{R}^3$, *Nonlinearity* **11** (1998), no. 4, 1037–1047

[15] F. Dumortier, S. Ibáñez and H. Kokubu, New aspects in the unfolding of the nilpotent singularity of codimension three, *Dynamical Systems* **16** (2001), 63–95.

[16] F. Dumortier, S. Ibáñez and H. Kokubu, Cocoon bifurcations in three-dimensional reversible vector fields, *Nonlinearity* **19** (2006), 305–328.

[17] E. Fontich and C. Simó, Invariant manifolds for near identity differentiable maps and splitting of separatrices, *Erg. Th. & Dyn. Systems* 10 (1990), 319–346.

[18] E. Fontich and C. Simó, The splitting of sepratrices for analytic diffeomorphisms, *Erg. Th. & Dyn. Systems* 10 (1990), 295–318.

[19] P. Gaspard, Local birth of homoclinic chaos, *Phys. D* **62** (1993), 94–122.

[20] N. K. Gavrilov, On some bifurcations of equilibria with a zero and a pair of purely imaginary eigenvalues, in *Methods of the Qualitative Theory of Differential Equations* (ed. E. A. Leontovich-Andronova), Gor'kov. Gos. Univ. Gorr'kij (1978), 33-40.

[21] P. Glendinning and C. Sparrow, Local and global behavior near homoclinic orbits, *J. Statist. Phys.* 35 (1984), 645–696.

[22] J. Guckenheimer, On a codimension two bifurcation, in *Dynamical Systems and Turbulence* (eds. D. A. Rand and L. A. Young), Lect. Notes Math., Vol. 898, 1981, Springer-Verlag.

[23] J. Guckenheimer and P. Holmes, *Nonlinear Oscillations, Dynamical Systems and Bifurcations of Vector Fields*, 1983, Springer-Verlag.

[24] A. J. Homburg, Periodic attractors, strange attractors and hyperbolic dynamics near homoclinic orbits to saddle-focus equilibria, *Nonlinearity* **15** (2002), 1029–1050.

[25] S. Ibáñez and J. A. Rodríguez, Shil'nikov configurations in any generic unfolding of the nilpotent singularity of codimension three on $\mathbb{R}^3$, *J. Differential Equations* **208** (2005), 147–175.

[26] N. Ishimura, Remarks on third-order ODEs relevant to the Kuramoto-Sivashinsky equation, *J. Differential Equations* **178** (2002), 466–477.

[27] J. Jones, W. C. Troy and A. D. McGillivary, Steady solutions of the Kuramoto-Sivashinsky equation for small wave speed, *J. Diff. Eq.* **96** (1992), 28–55.

[28] P. Kent and J. Elgin, A Shil'nikov-type analysis in a system with symmetry, *Phys. Lett. A* **152** (1991), 28–32.

[29] P. Kent and J. Elgin, Noose bifurcation of periodic orbits, *Nonlinearity* **4** (1991), 1045–1061.

[30] P. Kent and J. Elgin, Travelling-waves of the Kuramoto-Sivashinsky equation: period multiplyng bifurcations, *Nonlinearity* **5** (1992), 899–919.

[31] Y. Kuramoto and T. Tsuzuki, Persistent propagation of concentration waves in dissipative media far from thermal equilibrium, *Prog. Theor. Phys.* **55** (1976), 356–369.

[32] Y. A. Kuznetsov, *Elements of Applied Bifurcation Theory*, Third edition, 2004, Springer-Verlag.

[33] J. S. W. Lamb, M.-A. Teixeira, and K. N. Webster, Heteroclinic bifurcations near Hopf-zero bifurcation in reversible vector fields in $\mathbb{R}^3$, *J. Differential Equations* **219** (2005), no. 1, 78115.

[34] Y.-T. Lau, The "cocoon" bifurcations in three-dimensional systems with two fixed points, *Int. J. Bif. Chaos* **2** (1992), 543–558.

[35] F. Ledrappier, M. Shub, C. Simó, A. Wilkinson, Random versus deterministic exponents in a rich family of diffeomorphisms, *J. Stat Phys.* **113** (2003), 85–149.

[36] C. K. McCord, Uniqueness of connecting orbits in the equation $Y^{(3)} = Y^2 - 1$, *J. Math. Anal. Appl.* **114** (1986), 584–592.

[37] D. Michelson, Steady solutions of the Kuramoto-Sivashinsky equation, *Phys. D* **19** (1986), 89–111.

[38] J. Puig, C. Simó, Resonance tongues in the Quasi-Periodic Hill-Schrödinger Equation with three frequencies, *Regular and Chaotic Dynamics* **16** (2011), 62–79.

[39] S. V. Raghavan, J. B. McLeod and W. C. Troy, A singular perturbation problem arising from the Kuramoto-Sivashinsky equation, *Diff. Integ. Eq.* **10** (1997), 1–36.

[40] C. Simó, On the Hénon-Pomeau attractor, *J. of Statistical Physics*, **21** (1979), 465–494.

[41] C. Simó, Global Dynamics and Fast Indicators, in *Global Analysis of Dynamical Systems*, ed. H. W. Broer, B. Krauskopf, G. Vegter, pp. 373–390, IOP Publishing, Bristol, 2001.

[42] C. Simó, Some properties of the global behaviour of conservative low dimensional systems, in *Foundations of Computational Mathematics: Hong Kong 2008*, ed. F. Cucker et al. pp. 163–189, London Math. Soc. Lecture Notes Series **363**, Cambridge Univ. Press, 2009.

[43] C. Simó and A. Vieiro, Resonant zones, inner and outer splittings in generic and low order resonances of Area Preserving Maps, *Nonlinearity* **22** (2009), 1191–1245.

[44] C. Simó and A. Vieiro, Planar radial weakly-dissipative diffeomorphisms, *Chaos* **20** 043138 (2010).

[45] C. Simó, A. Vieiro, Dynamics in chaotic zones of area preserving maps: close to separatrix and global instability zones, *Physica D* 240 (2011), 732–753.

[46] F. Takens, Singularities of vector fields, *Publ. Math. IHES* **43** (1974), 47–100.

[47] W. C. Troy, The existence of steady solutions of the Kuramoto-Sivashinsky equation, *J. Differential Equations* **82**, (1989) 269–313.

[48] R. Vitolo, H. W. Broer, C. Simó, Quasi-periodic bifurcations of invariant circles in low-dimensional dissipative dynamical systems, *Regular and Chaotic Dynamics* **16** (2011), 155–185.

[49] K. N. Webster and J. Elgin, Asymptotic analysis of the Michelson system, *Nonlinearity* **16** (2003), 2149–2162.

[50] D. Wilczak, Symmetric heteroclinic connections in the Michelson system: a computer assisted proof (electronic), *SIAM J. Appl. Dyn. Syst.* **4** (2005) 489–514.

[51] T.-S. Yang, On traveling wave solutions of the Kuramoto-Sivashinsky equation, *Phys. D* **110** (1997), 25–42.